Properties of high-frequency seismic radiation : what they say on the earthquake fault structure and source process

A.A. Gusev

Institute of Volcanology and Seismology, Russian Ac.Sci. and

Kamchatka Branch, Geophysical Service, Russian Ac.Sci.

Petropavlovsk-Kamchatsky, Russia

Defining HF

~~(1): $f > 0.3$Hz~~

(2): $f > (5\text{-}10) f_{corner}$

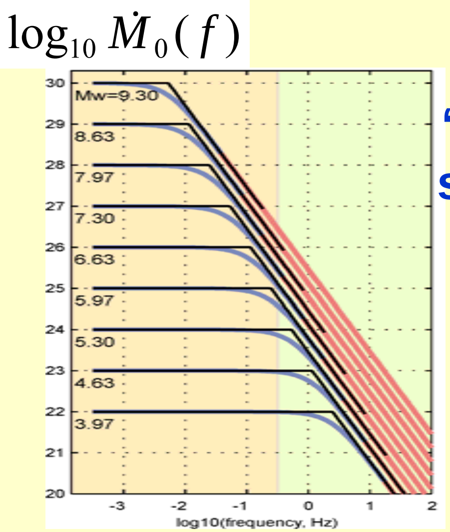

Scaling of "Source spectra"

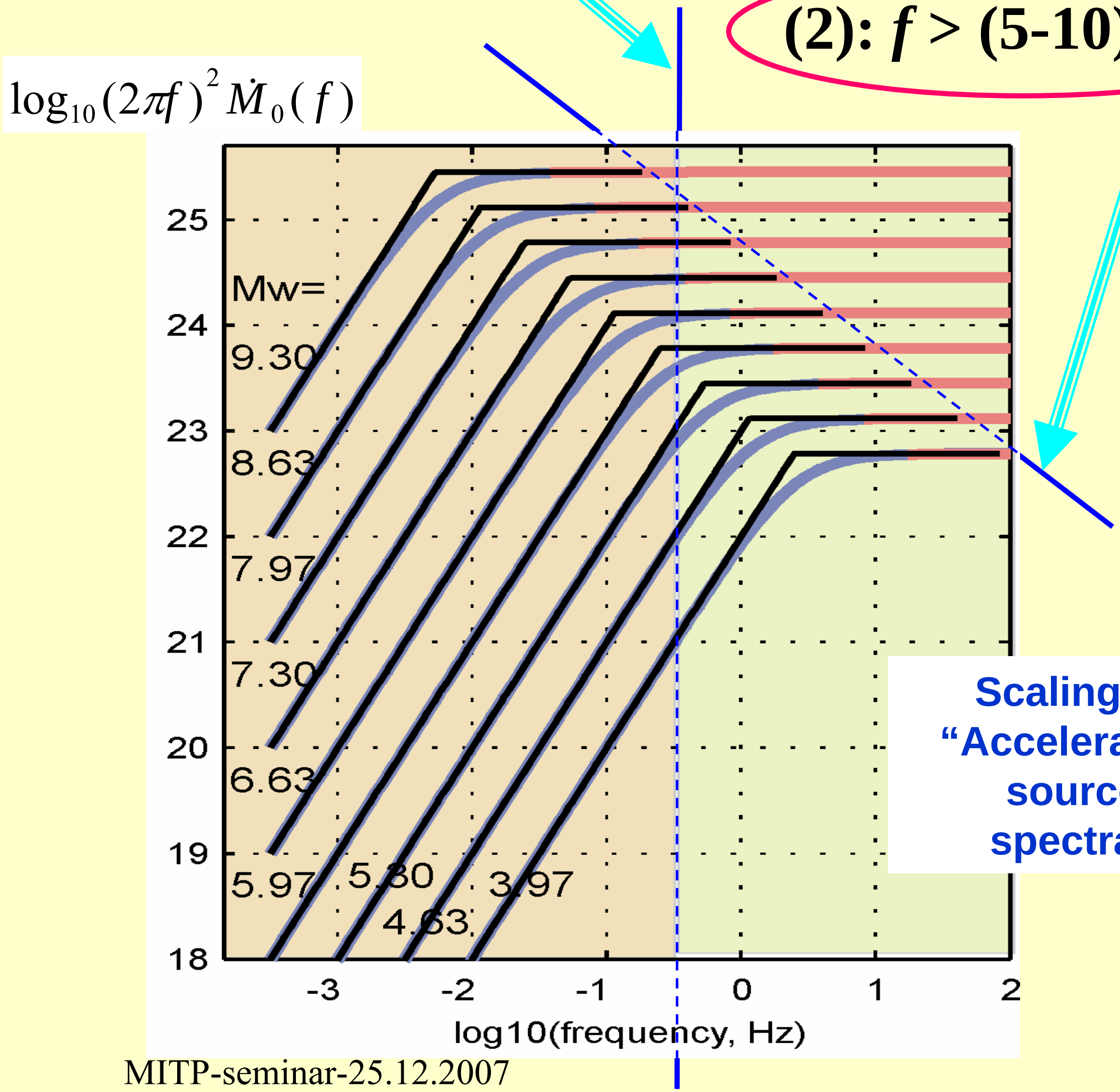

Scaling of "Acceleration source spectra"

HF radiation: properties, informal

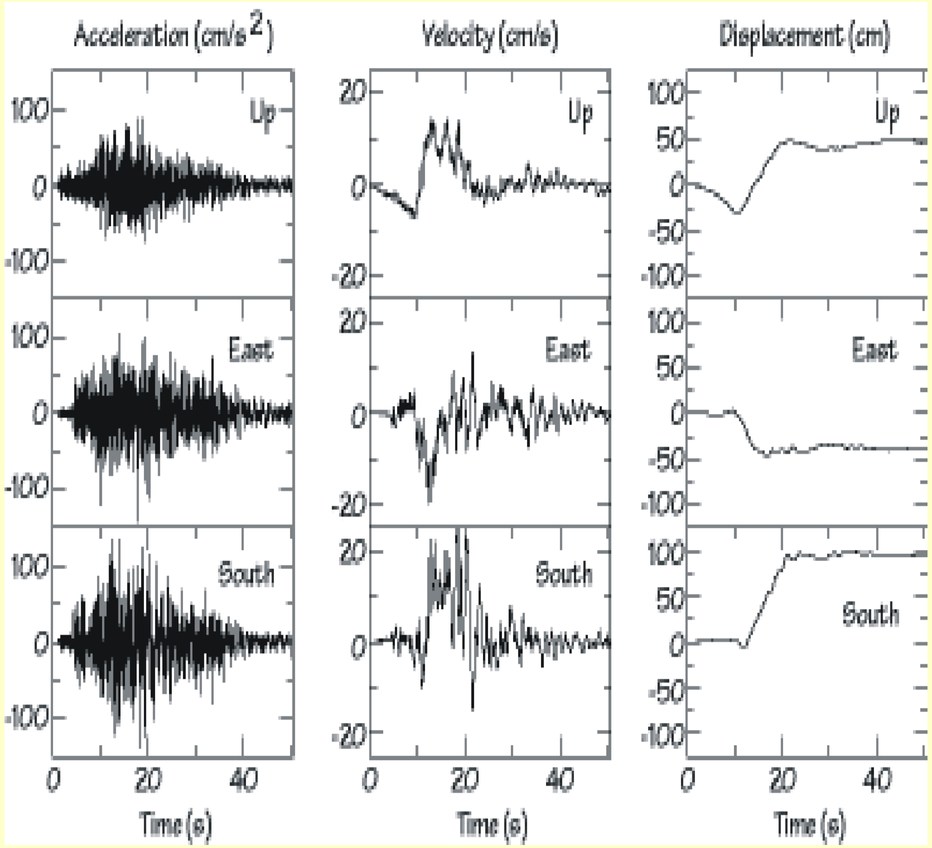

(1) appearance:

noise-like , random

(2) duration:

mostly same as that of LF pulse

(order of $1/f_c = T$)

(3) no harmonics,

smooth mean amplitude spectrum

Part 1
Specific properties of HF radiation

- **Random-like appearance of HF records**
- **Significantly deteriorated directivity as compared to LF**
- **Specific spectral shapes**

Random-like appearance of HF records

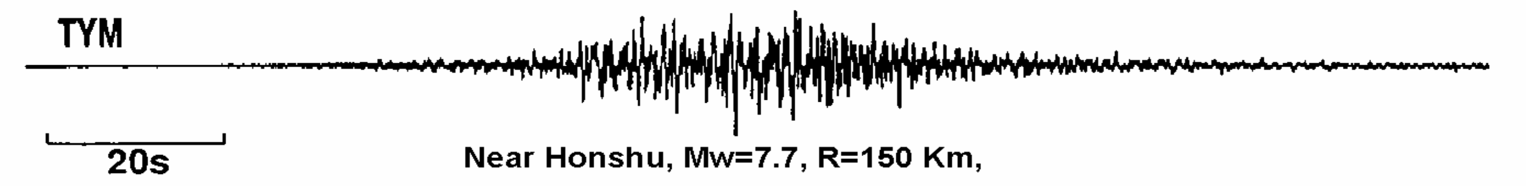

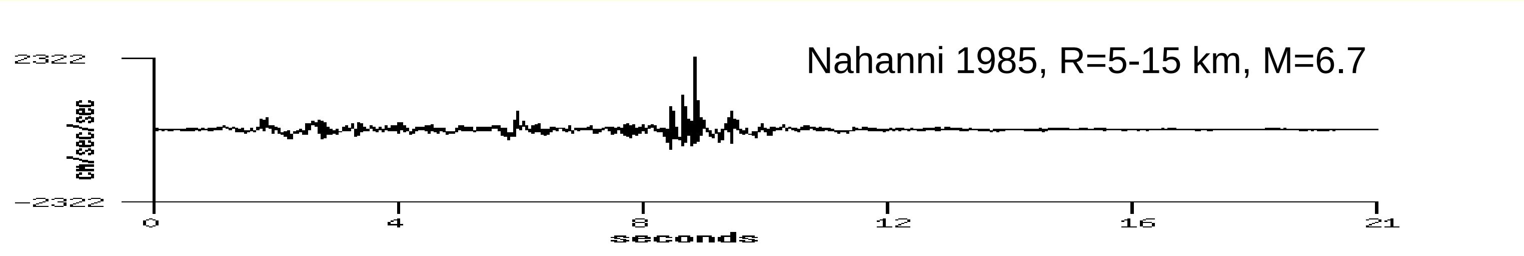

(1) Records of sufficiently large earthquakes, with source duration much longer than visual period, **look like segments of modulated/ "quasi-stationary" random process**

(2) At regional and teleseismic distances, HF records usually look like examples of **Gaussian** process (statistics of HF amplitudes is approximately Gaussian)

(2) At hypocentral distances less than 120-150 km; and specifically at distances below 30-40 km, obtained on rock ground, HF records usually look "spiky", they have **non-Gaussian, heavy-tailed** statistics

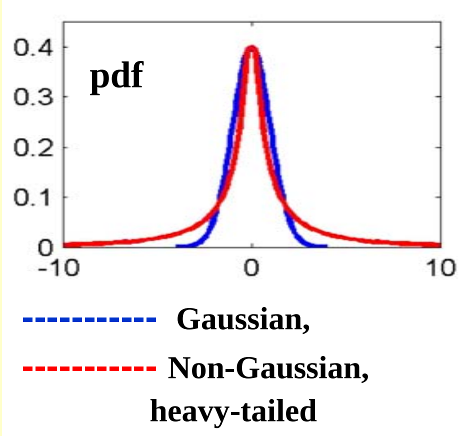

“Spiky” near-fault HF records: examples of accelerograms

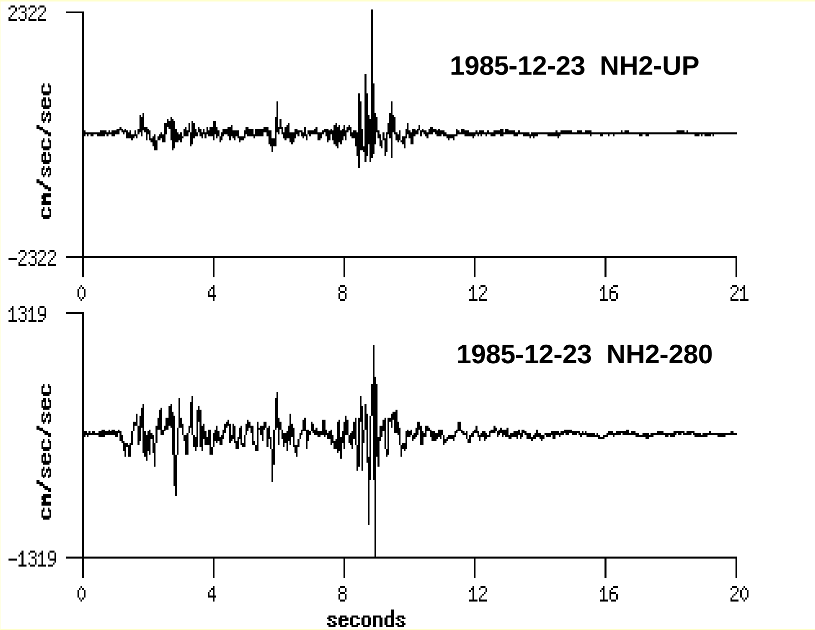

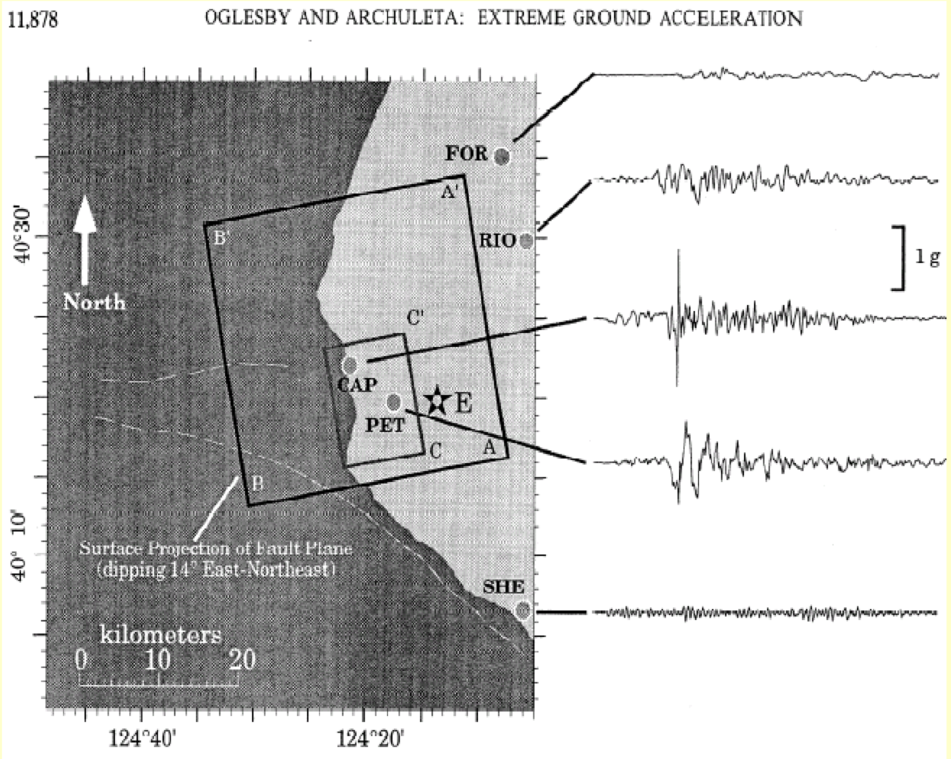

M=6.7 Nahanni EQ, 1985.12.23
R=5-15 km

M=7.0 Cape Mendocino/Petrolia
1992-04-25

Non-Gaussian peaks of accelerograms: 32 records, Δ-30-100 km, M>7,Mexico

original data:

event 1 **event 2**

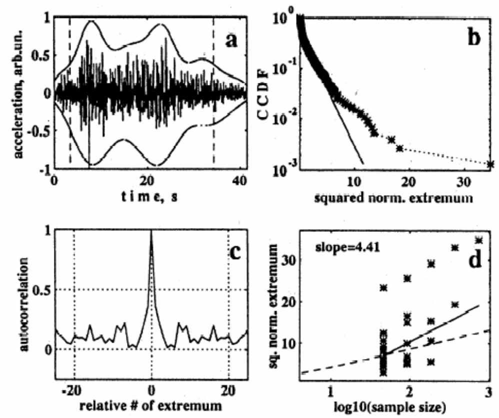

Figure 2. Statistical analysis of the original accelerogram of the September 21, 1985, event at the station UNIO, component N-S. (a) Time history. (b) CCDF of its squared extrema. (c) Autocorrelation of extrema. (d) Squared extremum versus sample size, that is the number of

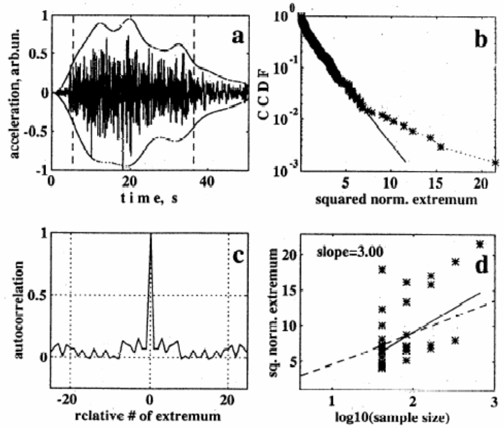

Figure 4. Same as Figure 2, for the September 19, 1985, event at the station CALE, component E-W.

Parameters analyzed:

(1) Peak factor:

$PF = a_{peak}/a_{rms}$

(2) $K = d\,PF^2 / d\ln N_{extrema}$

data passed through automatic gain control :

event 1 **event 2**

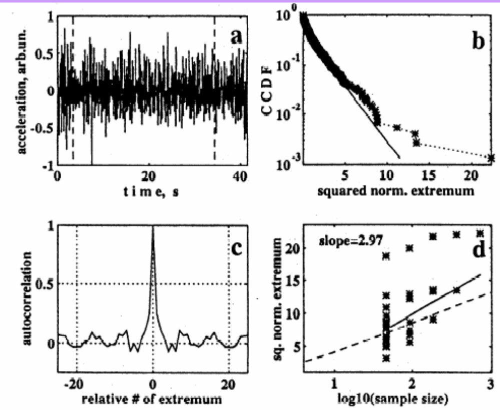

Figure 3. Same as Figure 2, except modified ("stationarized") version of the same accelerogram. The value f_{sm} = 0.06 Hz was used in the stationarization procedure.

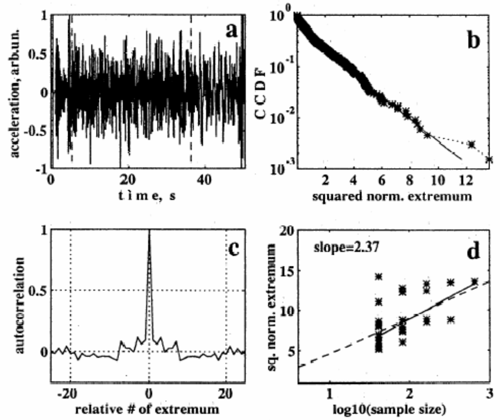

Figure 5. Same as Figure 3, for the September 19, 1985, event at the station CALE, component E-W.

Normalized parameters:

delta(K)=(K-K(Gauss))/σ(K)

delta(PF)=(PF-PF(Gauss))/σ(PF)

Non-Gaussian peaks of accelerograms, systematic study: 32 records, Δ-30-110 km, M>7, Mexico

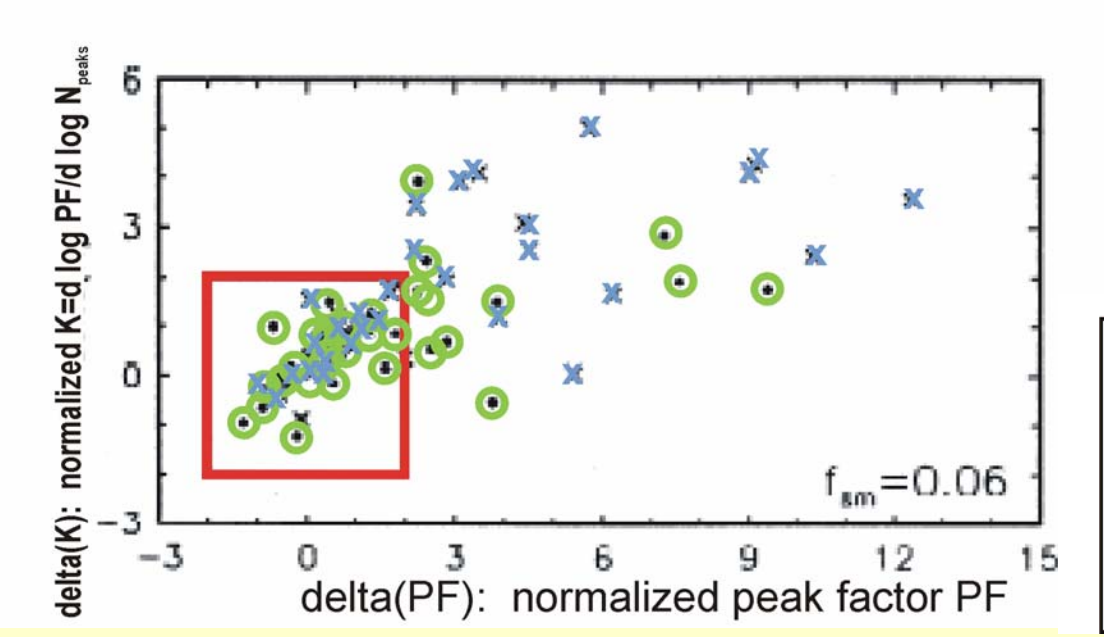

Peak factor: $PF=a_{peak}/a_{rms}$

PF growth rate: $K=d\ PF^2 / dlnN_{extrema}$

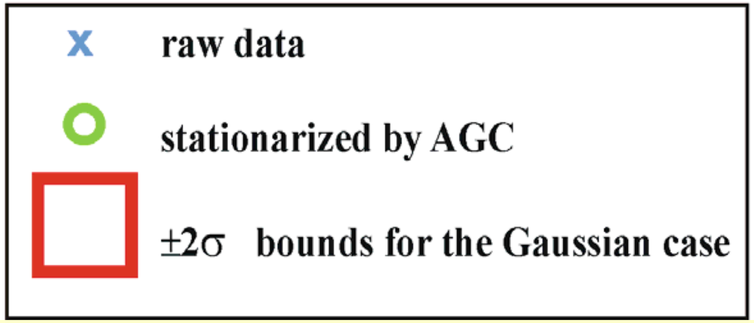

$PF=a_{peak}/a_{rms}$	delta(PF)=(PF-PF(Gauss))/s(PF)
$K=d\ PF^2 / dlnN_{extrema}$	delta(K)=(K-K(Gauss))/s(K)

Peak factors of teleseismic P wave deduced from mSKB:Mw relationship

$$mSKM = 0.35 \lg M_0 + const \approx 1.05 \lg T_{source}$$

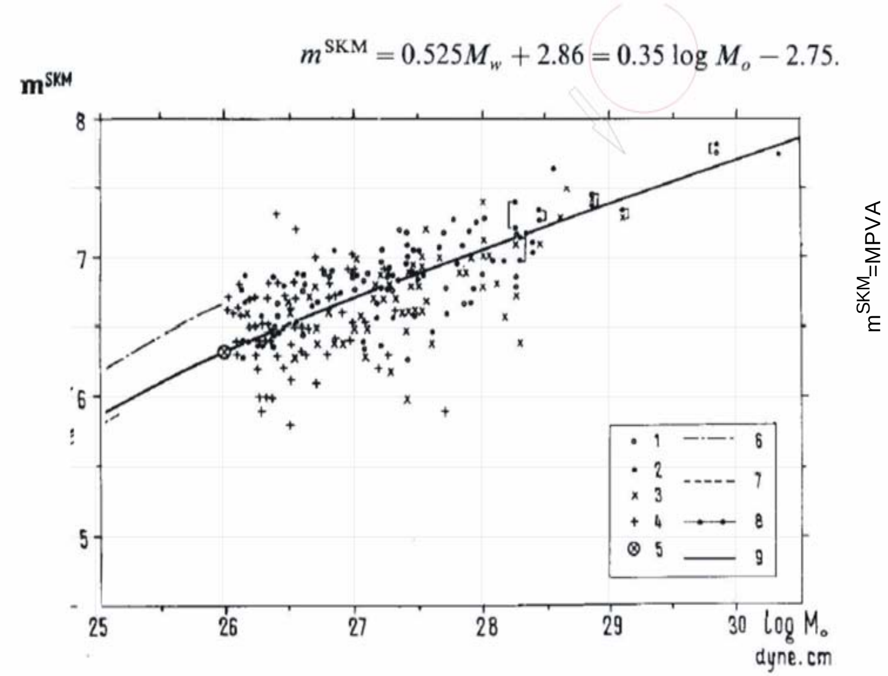

Figure 2

m^{SKM} vs M_o relationship. m_b, m_b^* and $\hat{m}_b$ data are also given, with correction of +0.18. 1—m_b^* after KOYAMA and ZHENG (1985); 2—$\hat{m}_b$ after HOUSTON and KANAMORI (1986) and ZHOU and KANAMORI (1987); 3—m^{SKM}, mostly from PURCARU and BERCKHEMER (1981); 4—m^{SKM} from ESSN catalogue and M_o from GIARDINI *et al.* (1985); 5—data centroids for m_b at given M_o from HAR; 6—"continental" trend of JOHNSON (1989); 7—"plate margin" trend of NUTTLI (1985); 8—trend for Kamchatka data partly using M_o from direct body waves; 9—accepted trend. Different estimates for the same event are indicated by a connection line.

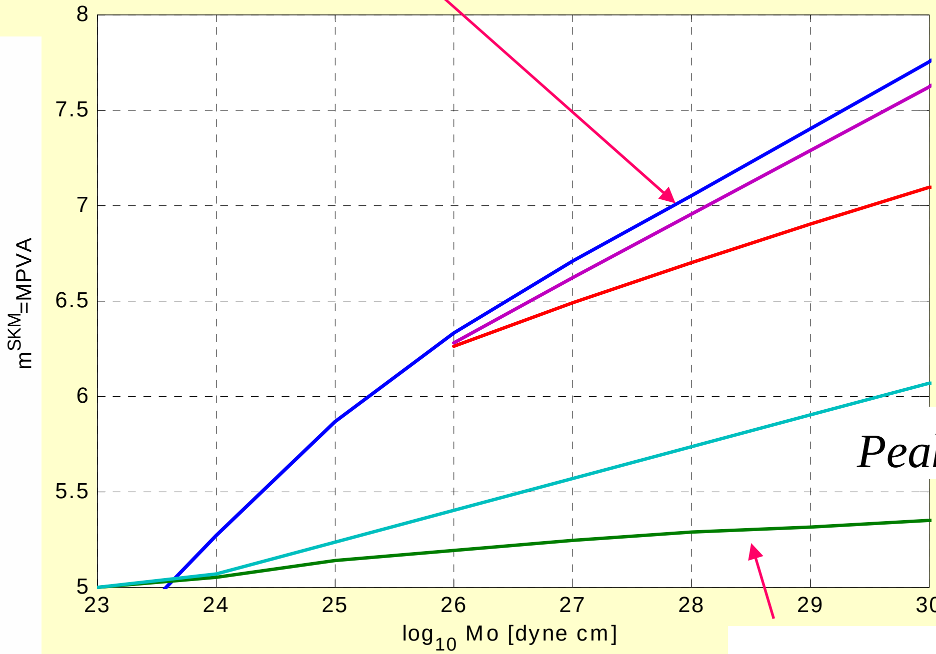

$$a_{rms} \times PF2$$

$$a_{rms} \times PF1$$

$$PeakFactor2 \propto t^{1/\alpha}$$

$$PeakFactor1 \approx (\ln t)^{0.5}$$

$$a_{rms} \propto M_0^{1/6}$$

Significantly deteriorated directivity as compared to low-frequency band: isoseismals

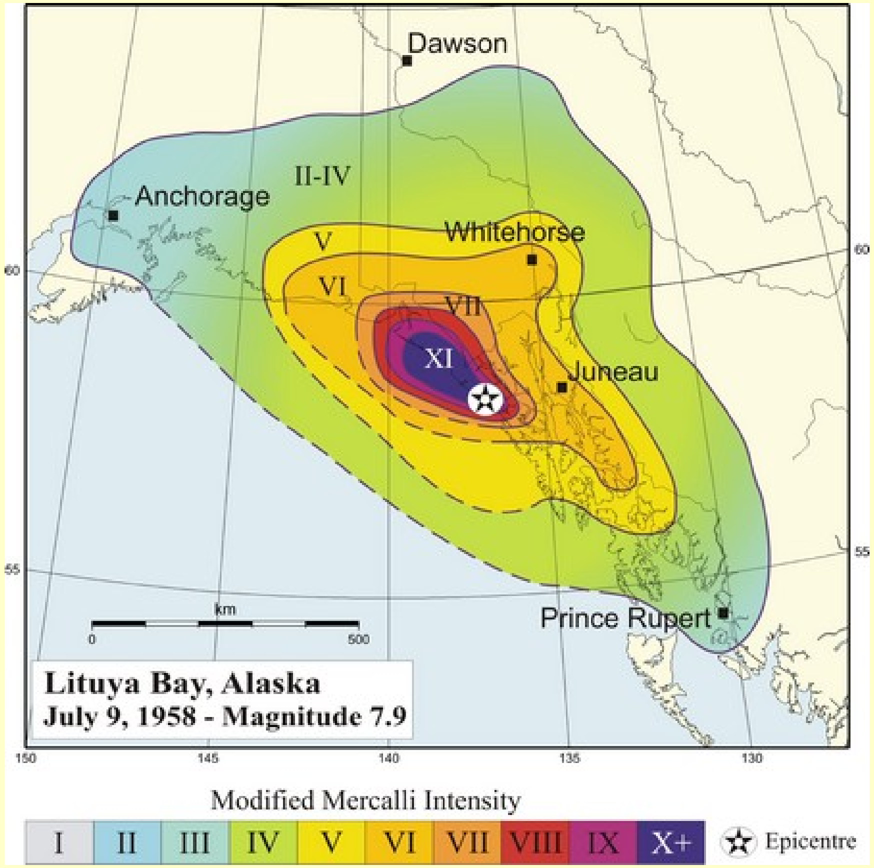

Even for elongated sources with unilateral ruptures, weak directivity is seen in macroseismic effects

asymmetric isoseismal shapes are mainly related
to lateral variations of attenuation and site effects

Significantly deteriorated HF directivity as compared to low-frequency band: spectra

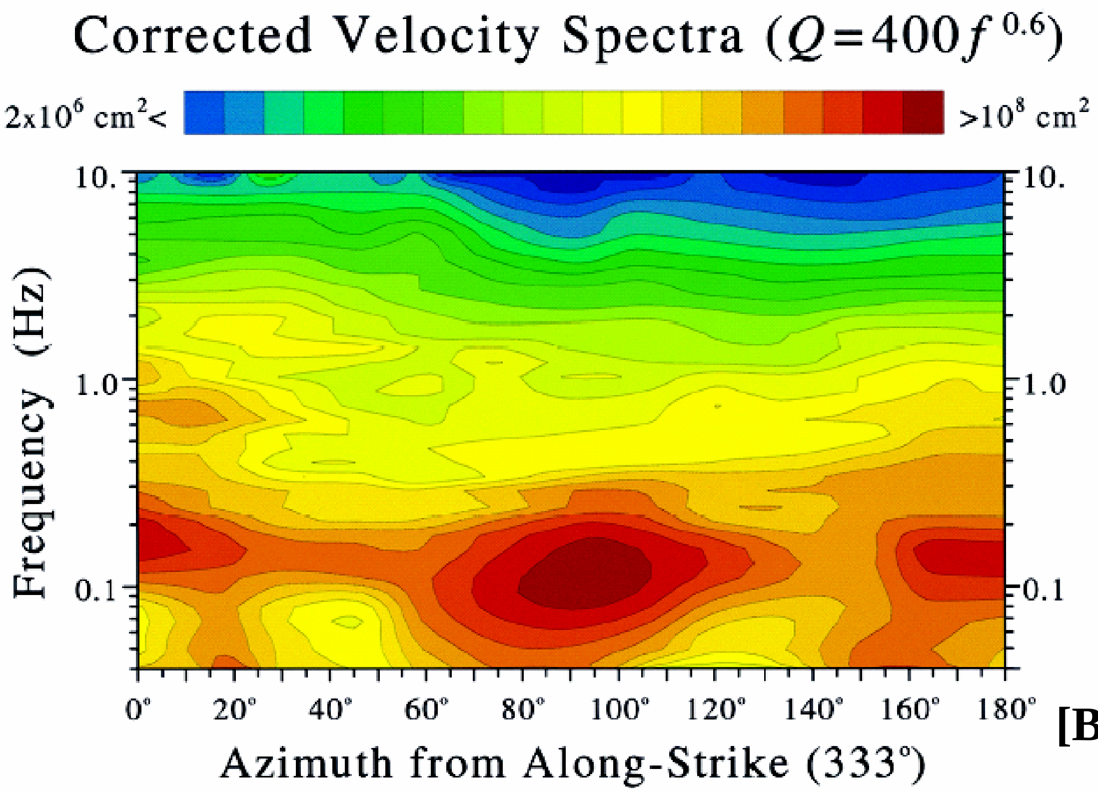

Figure 9. Corrected velocity spectra plotted as a function of the azimuth to the station. The clockwise and counterclockwise directions from NW along-strike are combined. There is some directivity to the NW at frequencies from 0.3 to 1.0 Hz, and less to the SE at frequencies from 0.3 to 0.6 Hz. Note the maximum at 90° and 0.1 Hz that indicates there is no directivity.

1999 M7.1 Hector Mine EQ
[Boatwright, Choy&Seekins 2002]

“Source” and body wave (amplitude) Fourier spectra: deterministic vs. “stochastic” viewpoint

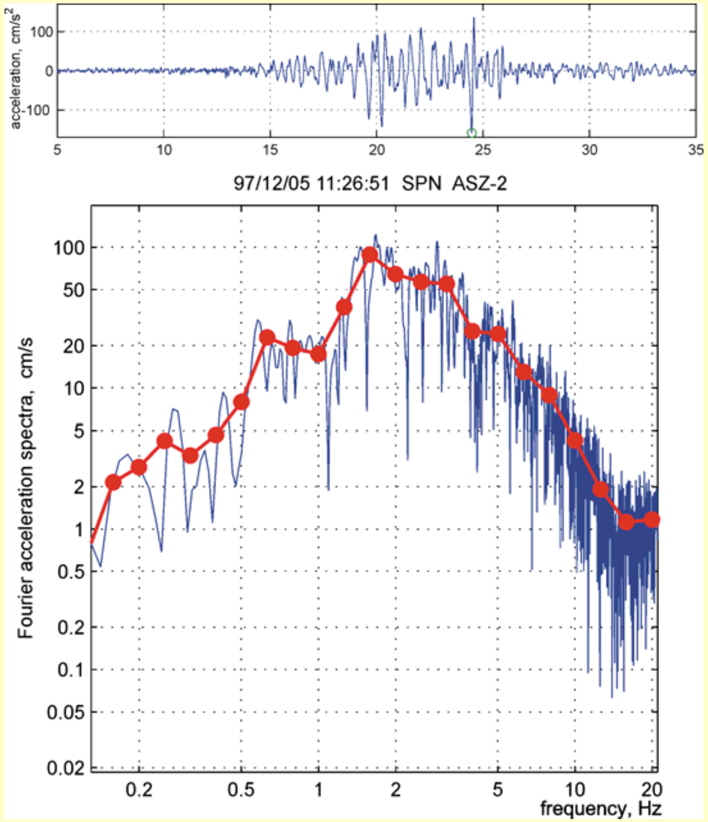

raw FS

smoothed FS

Deterministic view**:**

1. “Raw”, unsmoothed Fourier amplitude spectrum:
   the only real object
2. Smoothed Fourier amplitude spectrum:
   no clear meaning

“Stochastic” view (***meaningful at HF only***):

1. “Raw”, unsmoothed Fourier amplitude spectrum:
   sample function/realization of random process that underlies data
2. Smoothed Fourier amplitude spectrum:
   empirical estimate for $E^{0.5}(f)$
   (where $E(f)$ is energy spectral density)

$E^{0.5}(f)$ is a real subject of HF spectral models,
implicitly assumed to be a smooth function of frequency

Empirical/descriptive wideband spectral model [(Gusev 1983 and later work)]

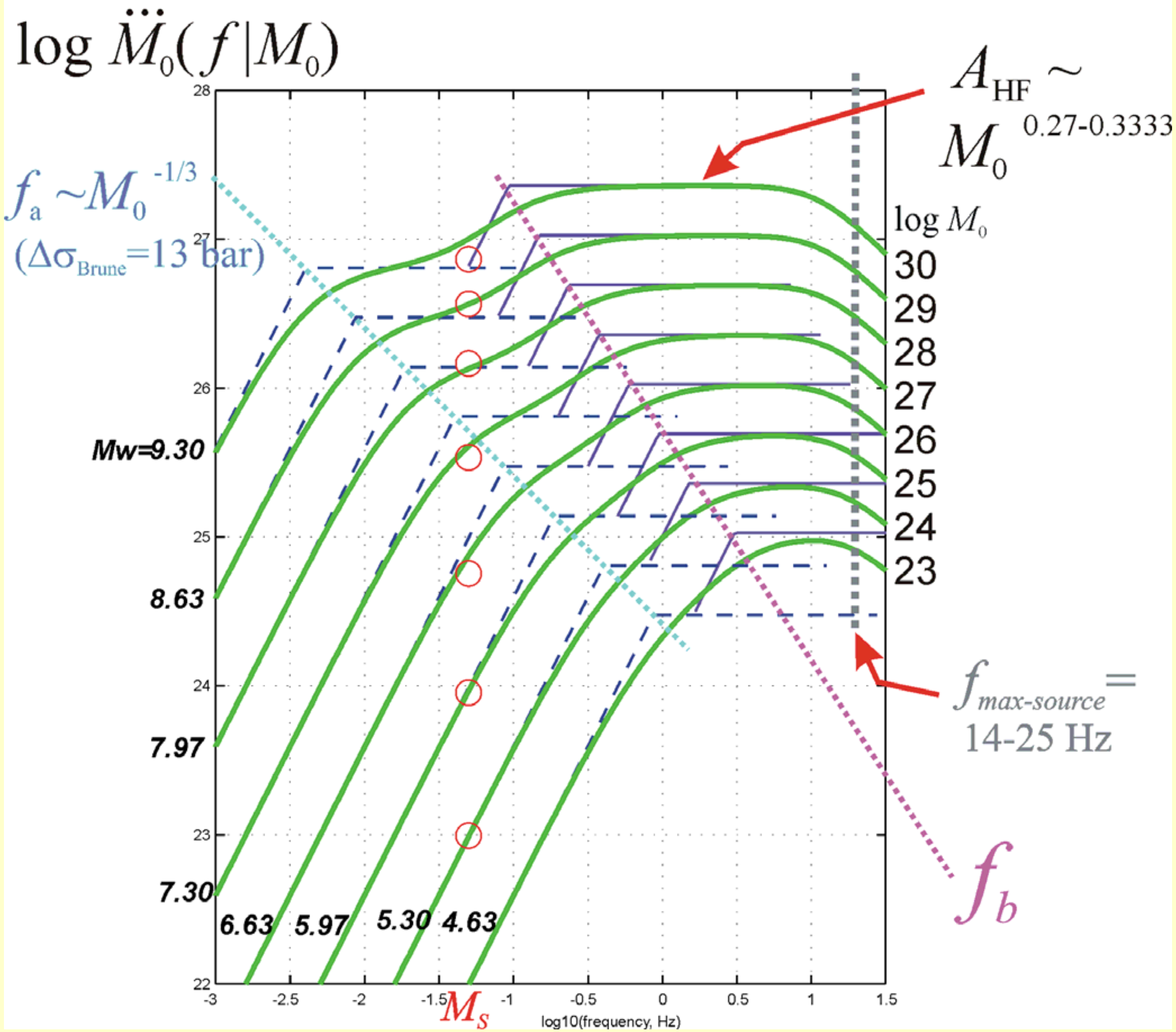

Schematic scaling based on work of Atkinson, Boore, Silva, Papageorgiou, Halldorfson, Dan, Irikura, Morikawa, Fujiwara

Empirical/descriptive wideband spectral model (2) [(Gusev 1983 and later work)]

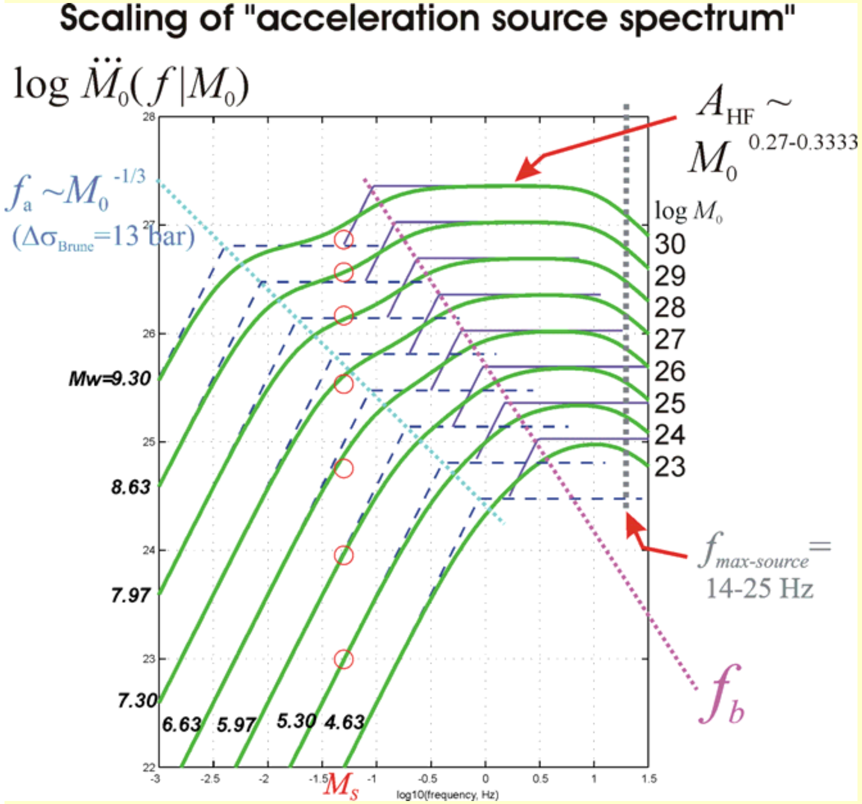

Main features

1. At LF, common scaling ($\boldsymbol{M_o} \propto \boldsymbol{f_a}^{-3}$) around common corner frequency $\boldsymbol{f_a}$ (like in ω^{-2} model)

2. Characteristic frequency $f_2 = \boldsymbol{f_b}$ around 0.3- 1 Hz, in addition to $f_{corner} = f_a$.
$\boldsymbol{f_b}$ is ***not proportional*** to $\boldsymbol{f_a}$: no simple similitude,

4. Flat HF [apprx 1-8 Hz] spectral level;
$\boldsymbol{A_{HF}} \propto M_o^{1/3}$ approx. (like in ω^{-2} model)

5. "Brune stress drops" based on $\boldsymbol{A_{HF}}$ are 3-6 times above those based on $\{\boldsymbol{f_a}, \boldsymbol{M_0}\}$

6. A source-related HF cutoff frequency, "$\boldsymbol{f_{max\text{-}source}}$", is present, in addition to attenuation-related $\boldsymbol{f_{max\text{-}att}}$; poorly known

Empirical spectral scaling laws with flat *accelerogram* spectra approximating *source* acceleration shapes

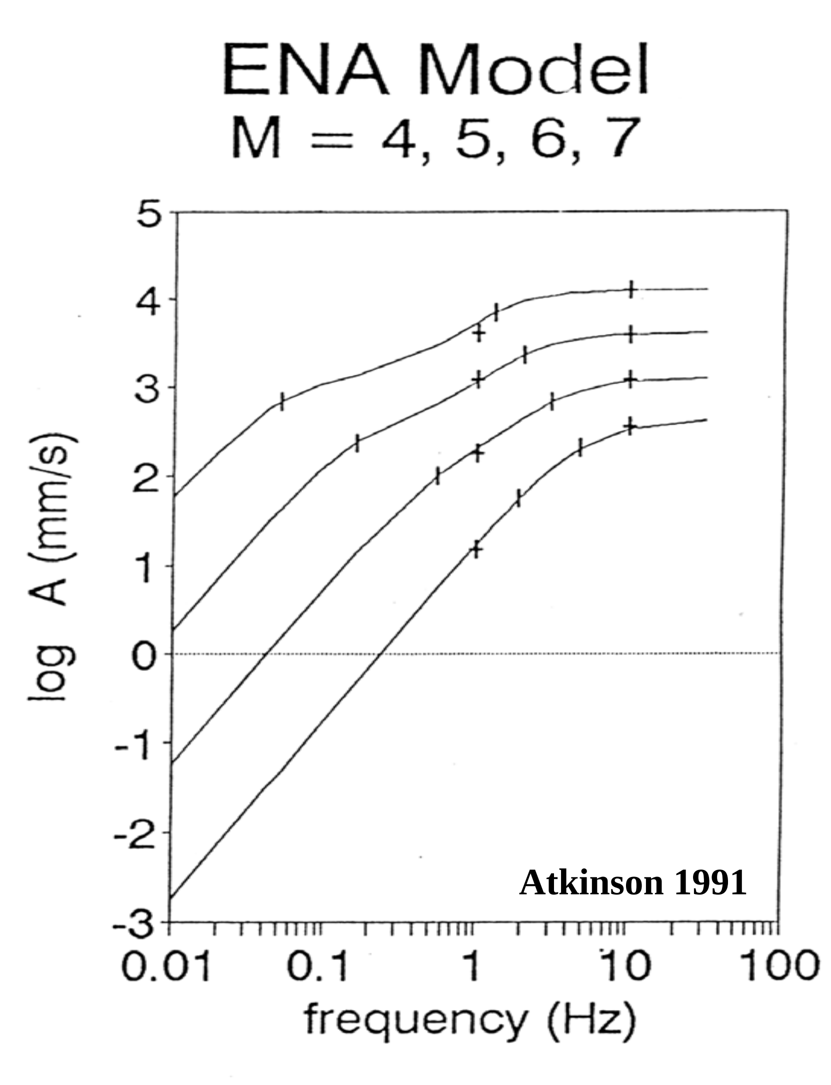

Atkinson 1991

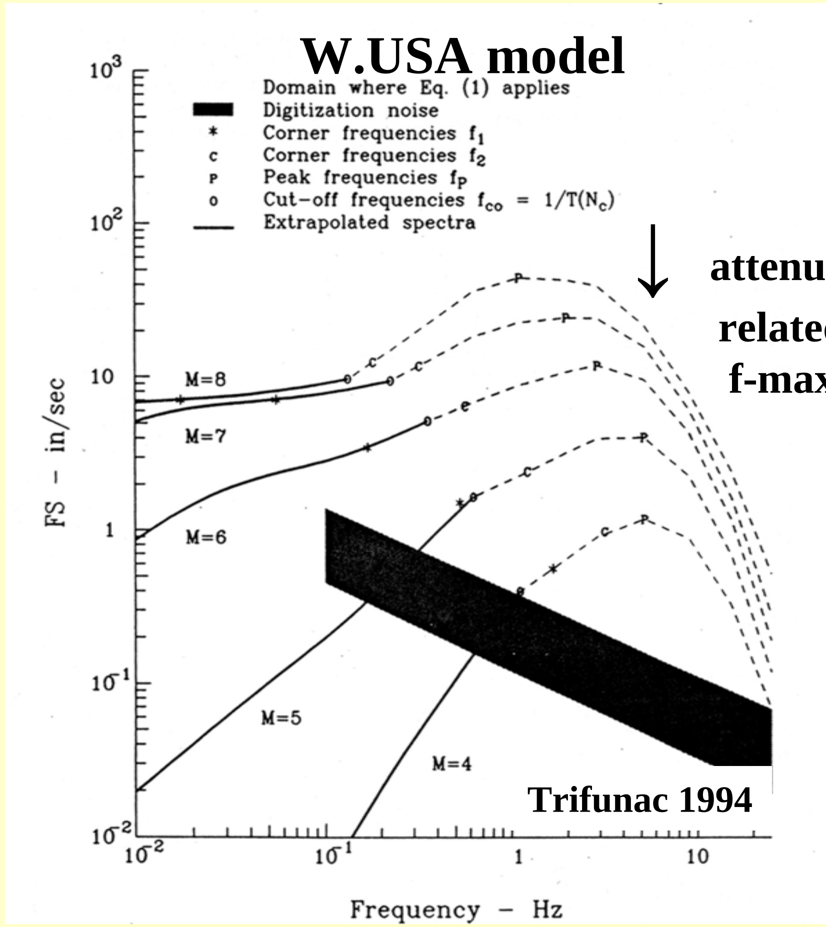

attenuation-related f-max

Trifunac 1994

Illustration of features of observed acceleration spectra

Source-related *f*-max: examples

Low to moderate magnitudes
Instruments in deep boreholes, eliminated attenuation-related f_{max}
Found, typically: source-related f_{max} between 10 and 25 Hz,

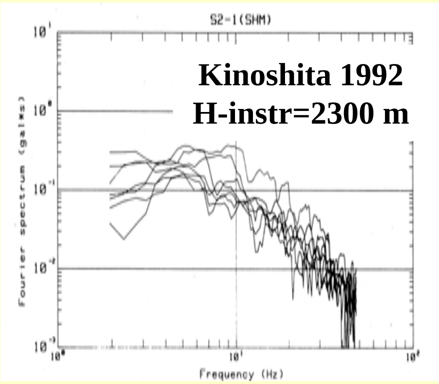

Kinoshita 1992
H-instr=2300 m

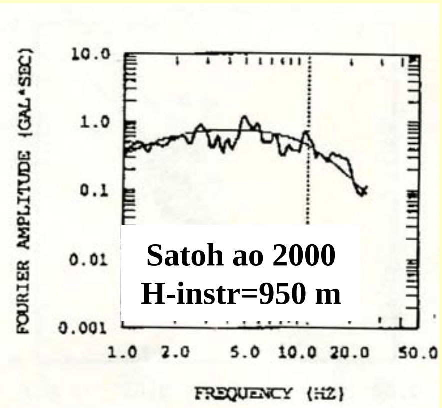

Satoh ao 2000
H-instr=950 m

Magnitudes 7-8
Pairs of earthquakes recorded at the same station
One of the two events have unusually low source-related $f_{max} \approx 3$ Hz
Attenuation-related f_{max} is present as usual
Can be eliminated by analysing spectral ratio

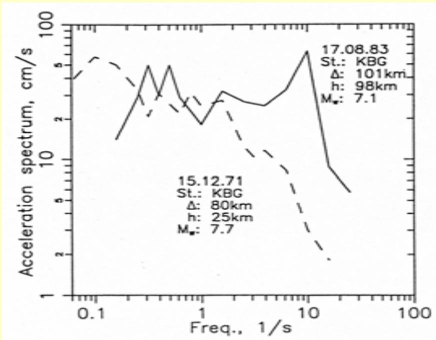

Gusev a.o. 1997

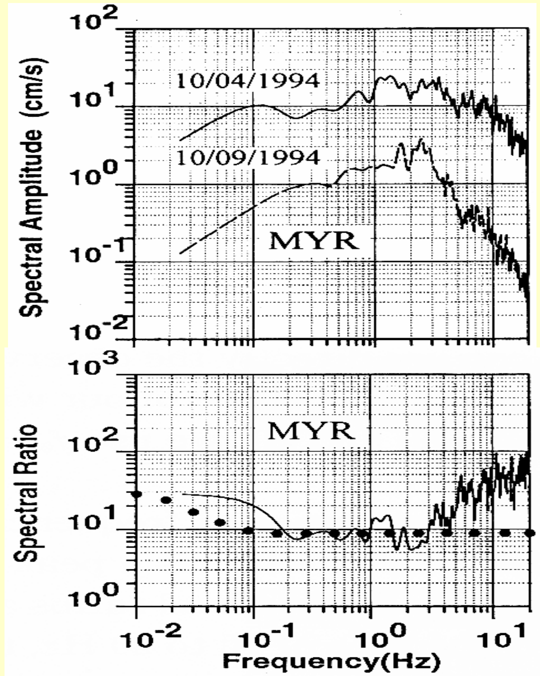

Sasatani 2001

Possible causes for HF properties

•Random-like record: random slip over fault surface $D(x,y)$
random local slip rate history $\mathrm{d}D(t|x,y)/\mathrm{d}t$
random "strength" (definition model-dependent)
??? random rupture tip velocity ???
generally: heterogeneous fault

•Spikes: .... Heavy-tailed stress drop/strength pdf *and/or* arcuate isochrones

•Deteriorated directivity:
.... fragmented, poorly defined rupture tip

•Spectral shape:...... many factors

Problem: how are related
local slip and **local HF radiation capability?**

Variant 1: **HF energy is generated mostly by large-slip patches, often called "asperities"**

Variant 2: **HF energy does not match high-slip patches;**
Variant 2a: **Rather, HF energy generation is "complementary" to slip**

Sources of information:
1: Degree of correlation between (1)displacement and (2)HF power signals from intermediate-depth earthquake

2. Degree of correlation between the results of inversion of space-time source structure in terms of (1)slip and (2)HF radiation

Comparing (1) body wave displacement pulse *and* (2) squared HF body wave velocity pulse from the same record of intermediate-depth earthquake

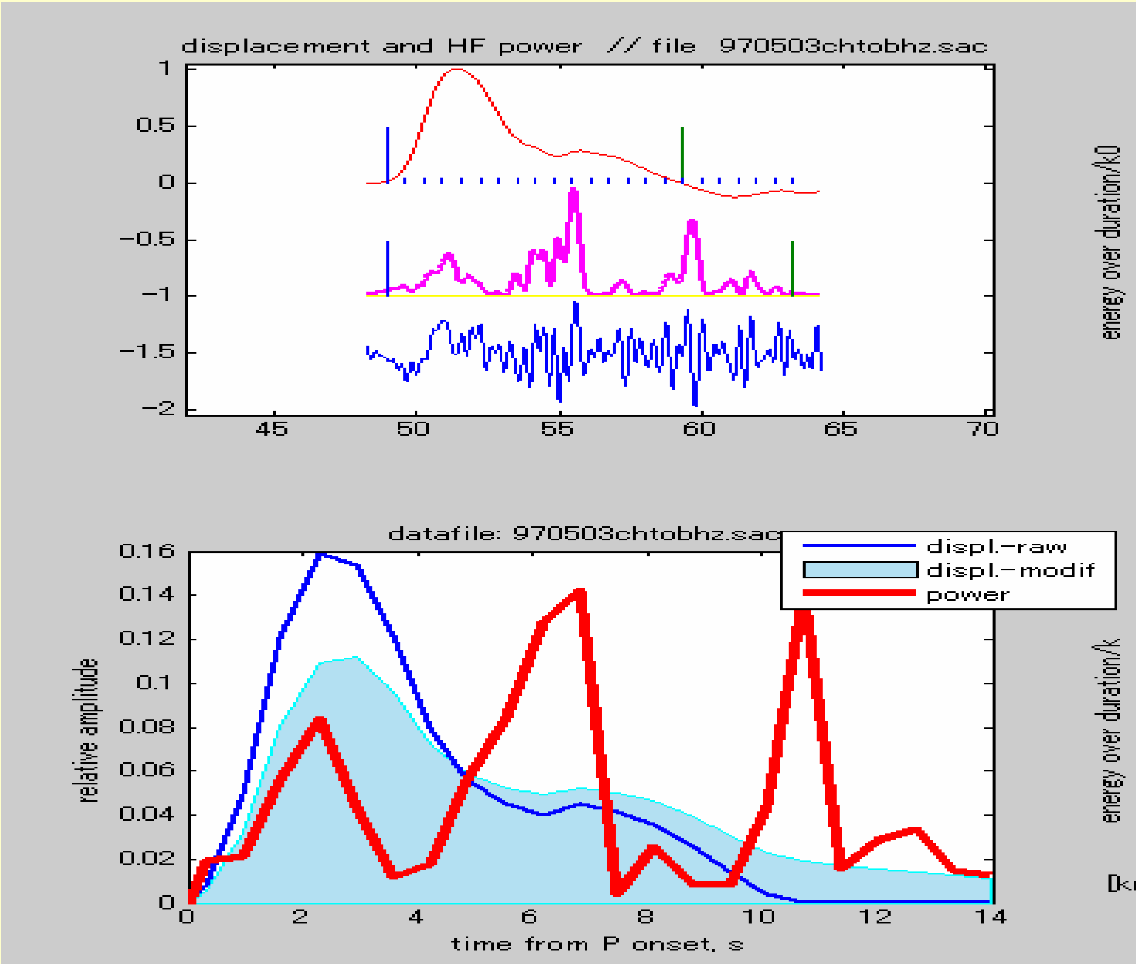

Gusev a.o. (2005) used
251 teleseismic P-wave records of GDSN
from 23 intermediate-focus earthquakes
(h=100-225 km)
with Mw=6.8-7.7.
As a HF signal, we use squared velocity
in the 0.5-2.5 Hz band

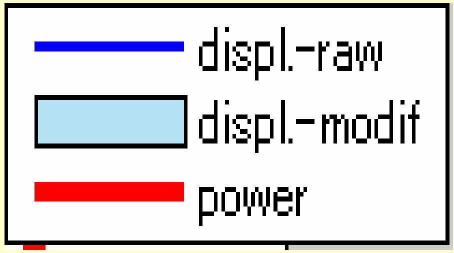

Examples of good and bad correlation between displacement and HF power

low-ρ cases

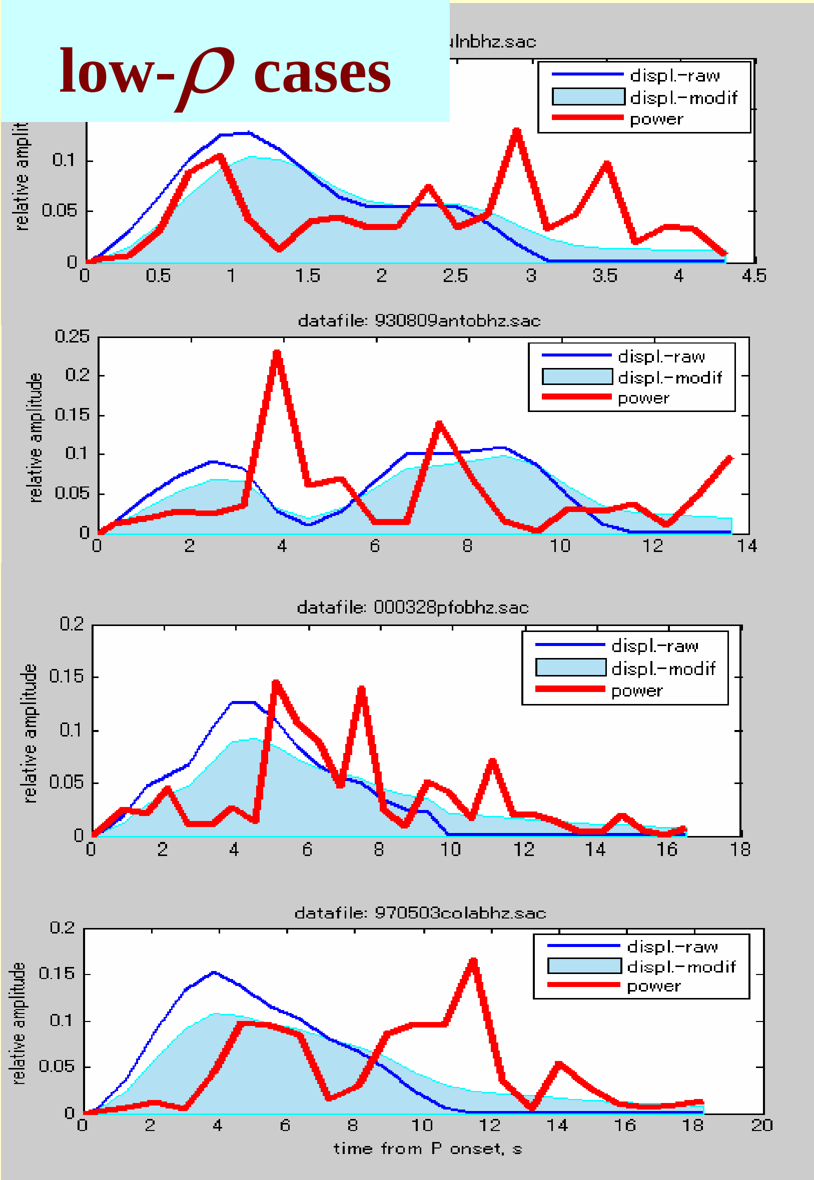

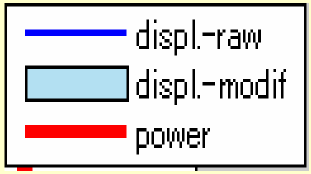

high-ρ cases

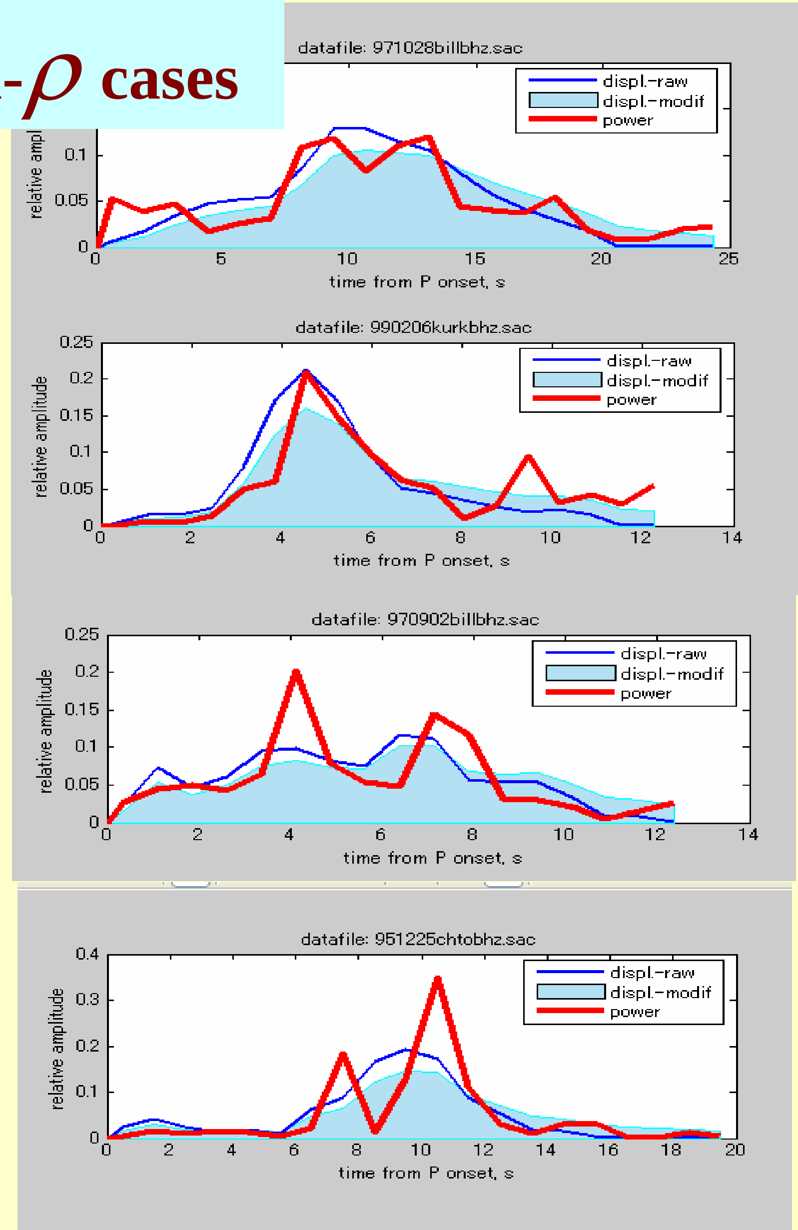

Relationship between local slip and local HF radiation capability-example

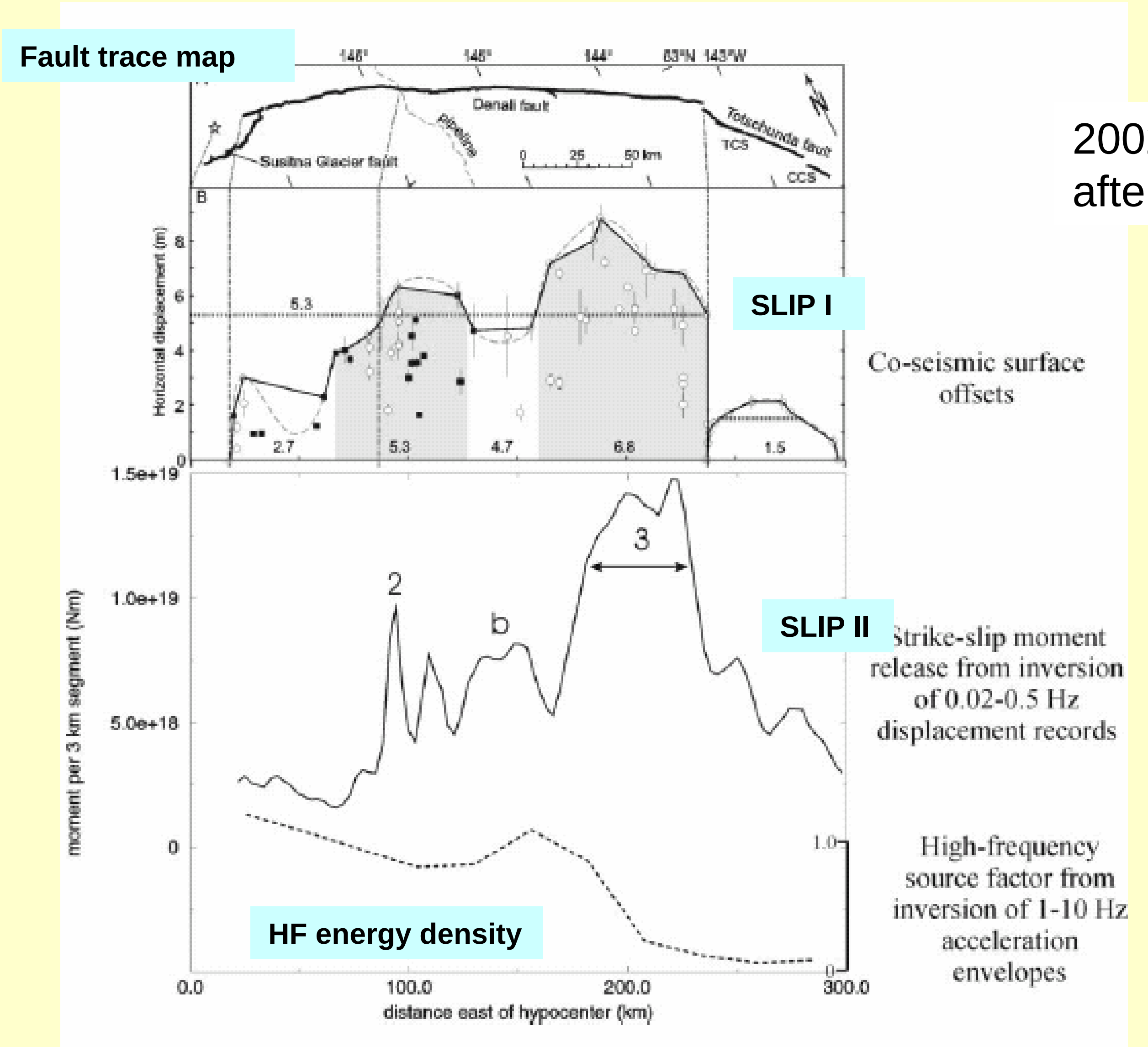

2002, M7.7, Denali, after Frankel 2004

Inversion of fault HF radiation capability ("luminosity") in space and time

Traditional inversion for slip D:

forward problem: $u[\text{at receiver}] = G[\text{medium}] * D[\text{at source}]$

inversion: $D[\text{at source}] = G^{-1}[\text{medium}] * u[\text{at receiver}]$

Inversion for luminosity L:

forward problem: $P[\text{at receiver}] = G'[\text{medium}] * L[\text{at source}]$

inversion: $L[\text{at source}] = G'^{-1}[\text{medium}] * P[\text{at receiver}]$

where: P is wave power at receiver in a certain HF band $\Delta f = [f_1, f_2]$

L is source luminosity in HF band Δf

G' is medium response for power in HF band Δf

Condition: P, G' and L can be treated as segments of modulated/ "quasi-stationary" random process

Relationship between local slip and local HF radiation capability-example 1

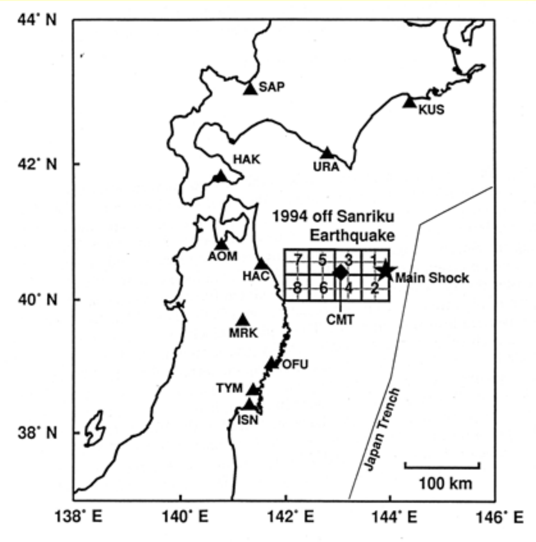

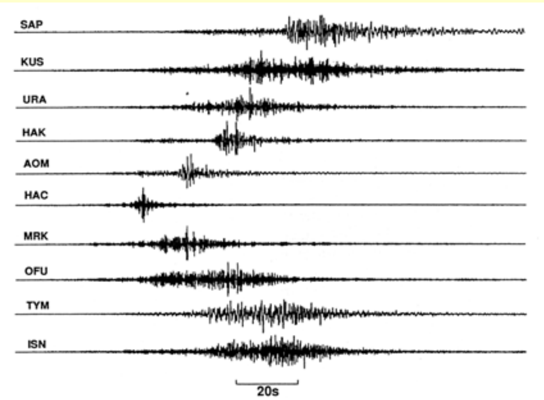

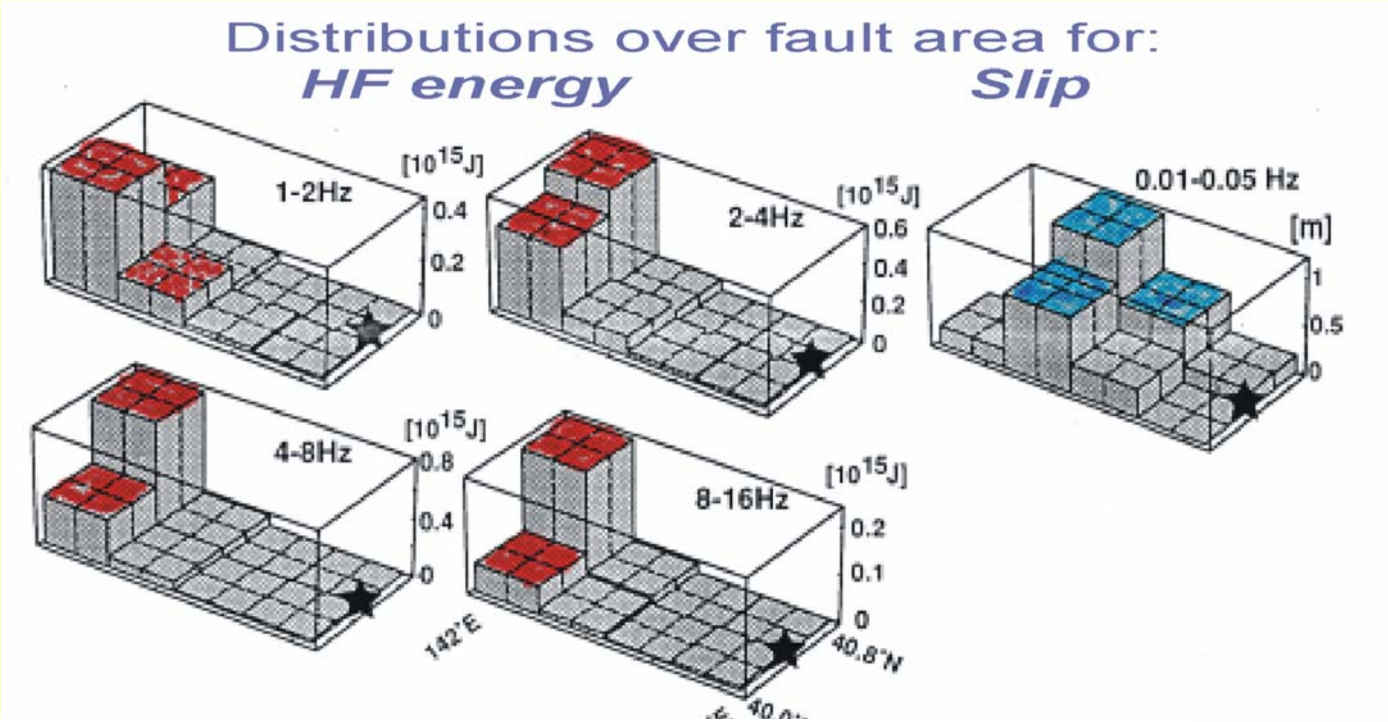

1994, M7.7, off Sanriku, Japan; inverted by Nakahara a.o. (1998)

Summary on slip-HF energy relationship

1. No clear tendency to match between high-slip and high-luminosity areas
2. “Complementary” behavior is common
3. Coefficient of correlation varies widely, roughly between 0.3 and 0.9

Part 2.
Models proposed for broad-band source radiation
(descriptive/phenomenological models
no dynamics, often poor tectonophysics)

1. Composite sources :
   consisting of subsources of various nature
   (including ones used in engineering-seismology practice)

2. Random function models
   (less developed, no applications)

A.Composite sources

(1) Cracks/patches, overlapping

<<tectonophysically impossible>>

<<works for accelerogram simulation>>

(2) Cracks/patches, non-overlapping/tiling,

a: with non-breakable barrier around each patch

<<tectonophysically improbable>>

<<works for accelerogram simulation>>

b: with barriers that break during current earthquake

<<tectonophysically imaginable,
dynamically doubtful>>

<<not tested for accelerogram simulation>>

(3) Small strong asperities

<<tectonophysically reasonable,
dynamically acceptable>>

<<not tested for accelerogram simulation,
acceptable accelerogram spectra and statistics>>

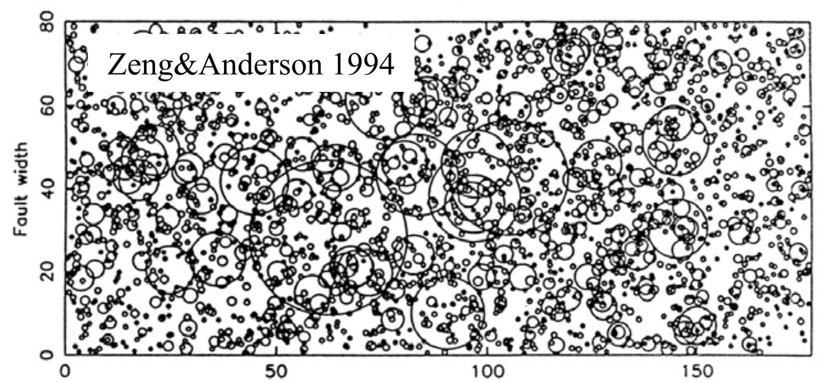

Zeng&Anderson 1994

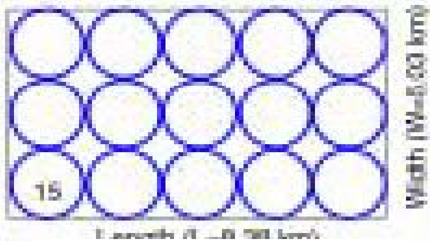
Aki&Papageorgiou 1983

Irikura 1994

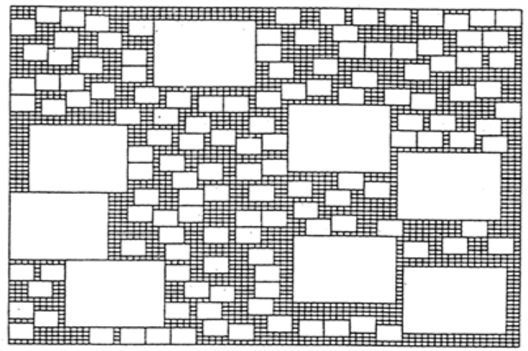

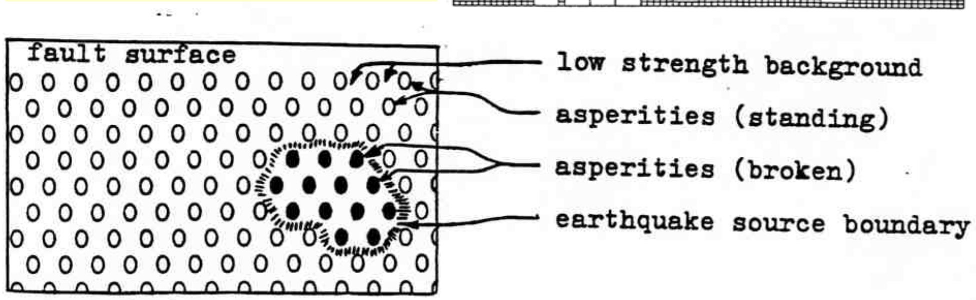

Gusev 1990 following Das& Kostrov 1988

B. Random function models

Random function in space-time specified by
correlation function over x,y,t; or by power spectrum over k_x,k_y,f

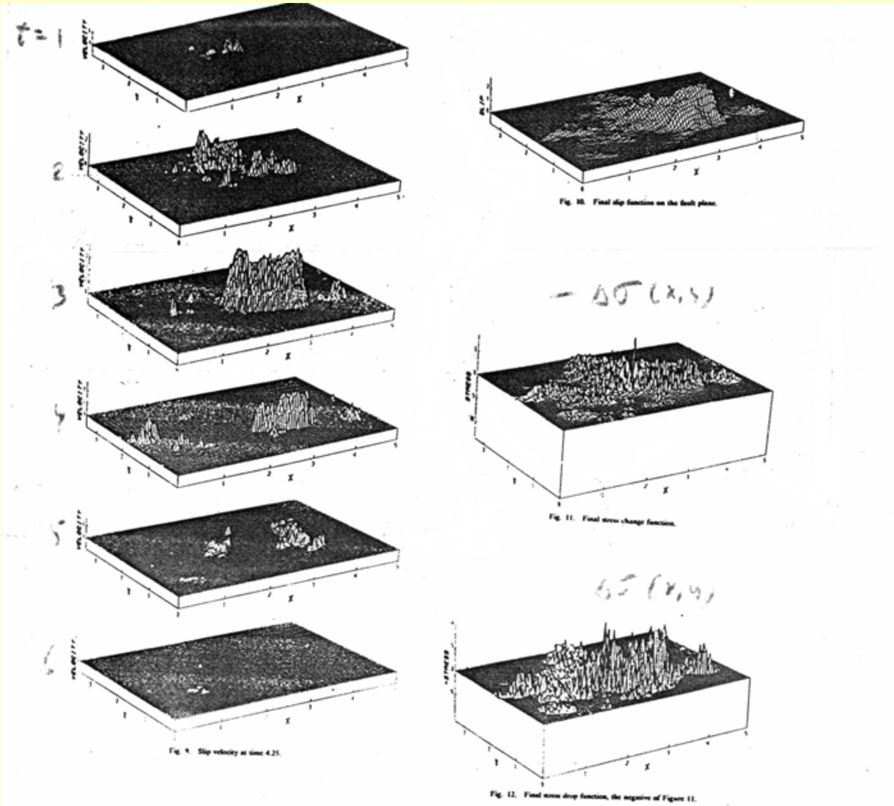

Haskell-Aki 1966-1967:
HF - HK source specified by, effectively,
power-law spectrum in in space-time
<<causal rupture with rupture front
no spikes
partly inconsistent mathematically
numerically not tested, >>

Andrews 1981:
HF - HK source specified by
power-law spectrum in space-time
<<no causality, no rupture front
no spikes
mathematically consistent
numerically tested>>

Part 3. On possible mechanisms responsible for properties of HF radiation

A. Heterogeneity of strength,
heavy-tailed strength statistics: probably related to

non-planar, rough, multiscaled fault geometry

non-planar, rough, multiscaled fault geometry
is a characteristic, universal property of geological faults
as they exist in the Nature;
at least, geophysicists must follow this empirical fact,
eventually, they must create models that reproduce it

Strength heterogeneity from fault wall relief
(1) free space/gap is formed

3D composite topography of fault walls [fault_gap(x,y)]
contacts: red "lakes" where gap=0 and normal stress $\neq 0$
all strength localized at "lakes"

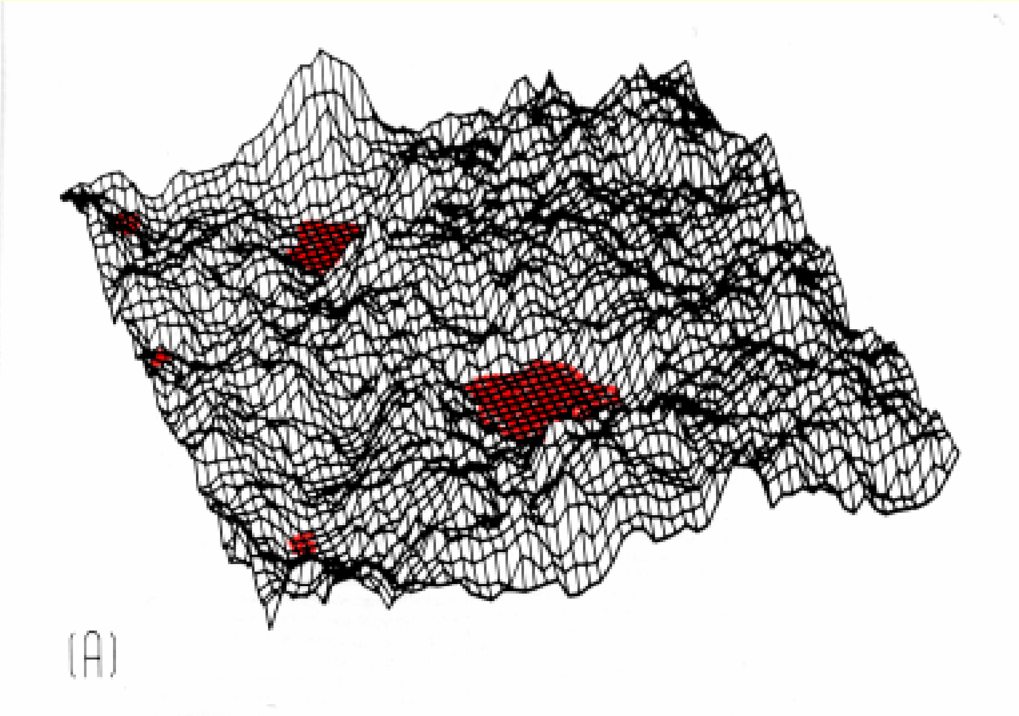

Attractive model:
explains:
- randomness of HF signal
- strong local patches,
- non-Gaussian accelerograms

Difficulty:
needs sufficient pore pressure to create free volume at depth

Strength heterogeneity from fault wall relief
(2) free-space/gap is closed by confining pressure; fault walls contact over entire area

Rough, *fractally curved* fault (Dieterich 2000)

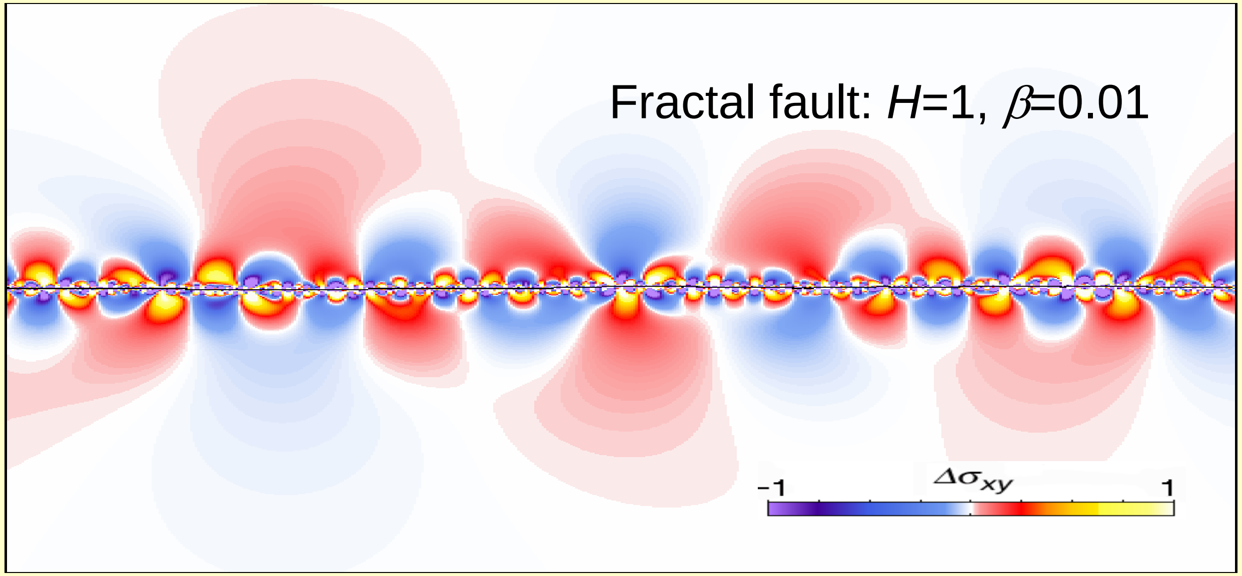

Attractive model:
explains:
- randomness of HF signal
- strong local patches

not explained:
- non-Gaussian accelerograms:

Difficulties of strength heterogeneity models based on fault wall relief

Stress concentrations on a rough geological fault
(and/or amount of free volume)
increase with each earthquake;

their relaxation/yielding is assumed only abstractly:
the particular way of relaxation remains unclear

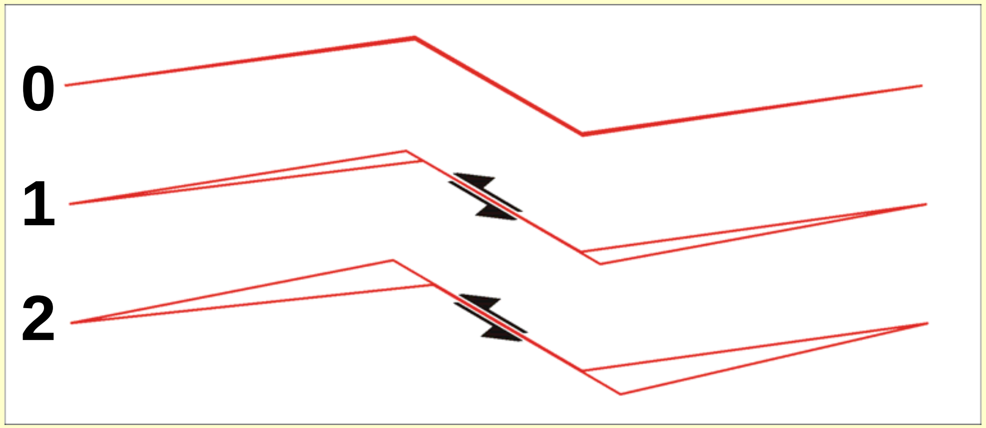

Strength heterogeneity related to *non-monolithic* non-planar fault walls

Fault is angular, bifurcating/branching
Medium consists of many discrete monolithic blocks (Andrews 1994)
Stress concentration minimal for infinitesimal slip; may be large for finite slips

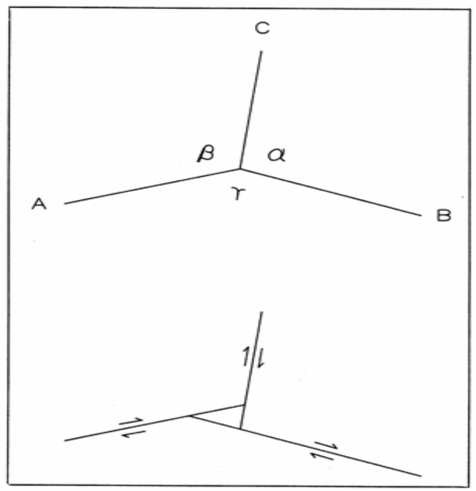

Fig. 1. Top: a junction of fault segments A, B, and C. The opposite angles α, β, and γ are each less than 180°. Bottom: rigid-body displacement at the junction consists of slip in the same sense on the three fault segments, and a void opens.

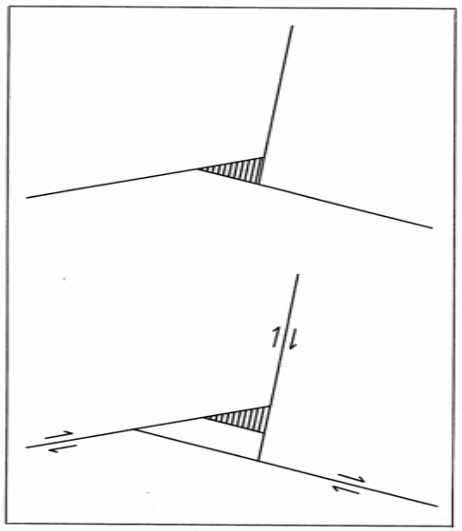

Fig. 4. Top: the triple junction shown in the bottom of fig. 1 with the void filled with fluid or remineralized. Bottom: another increment of slip produces a larger increment of void volume.

Attractive model:
explains how stress concentrations can relax and disappear from a rough surface of a sliding fault

Never was sufficiently developed to show its real potential;

Problem: mechanics of finite slip and related stress relaxation not developed

no fault gap; *branch faults* at each main-fault turn
no strong stress concentrations related to fault shape
splitting of dislocations pumps a fraction of seismic moment to branch faults
strength still highly heterogeneous because finite amount of slip is incompatible and fresh material must be crushed:

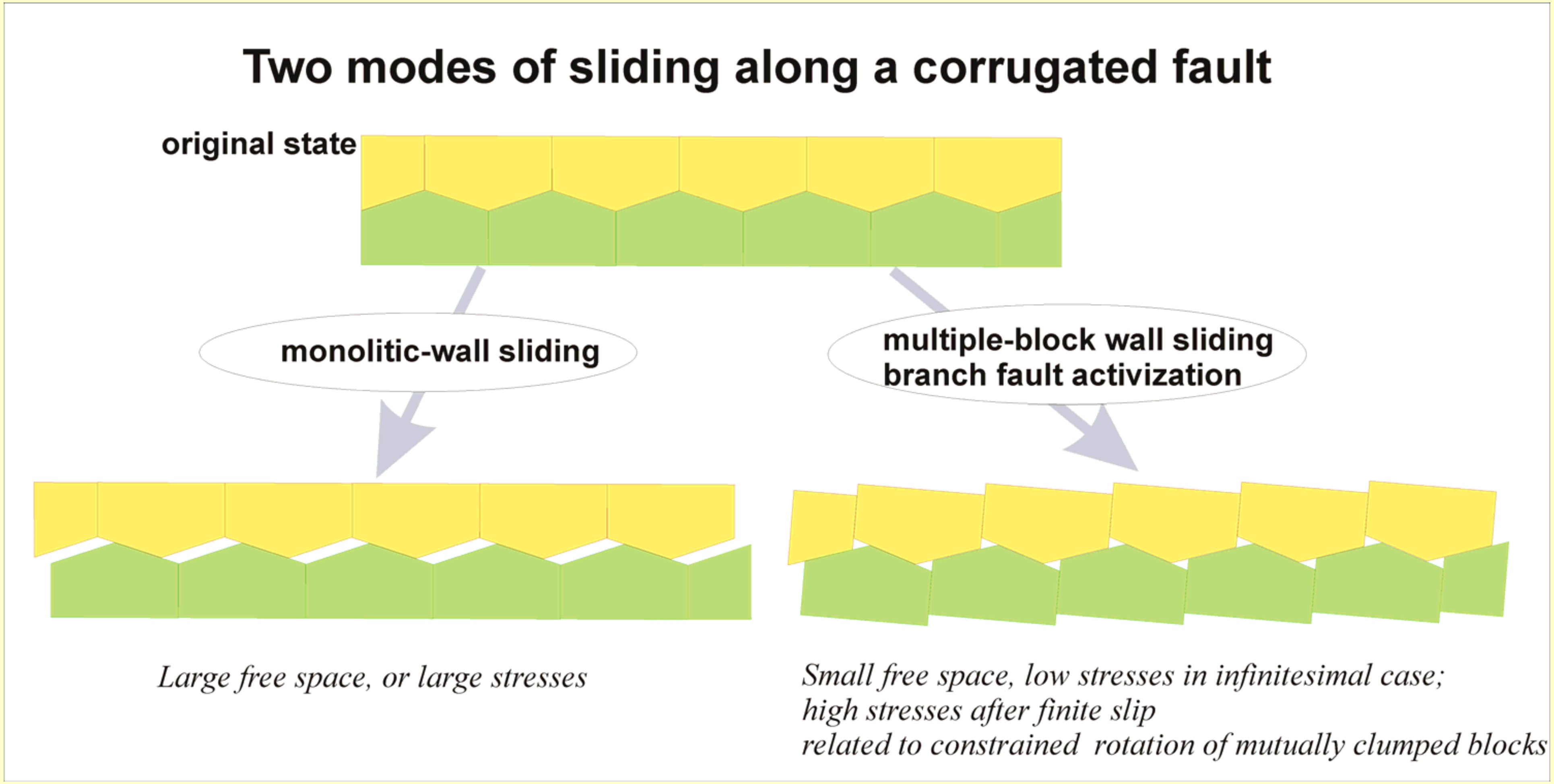
Two modes of sliding along a corrugated fault
original state
monolitic-wall sliding
multiple-block wall sliding
branch fault activization
Large free space, or large stresses
Small free space, low stresses in infinitesimal case;
high stresses after finite slip
related to constrained rotation of mutually clumped blocks

Examples of coseismic/early postseismic motion along branch/ secondary faults from INSAR images

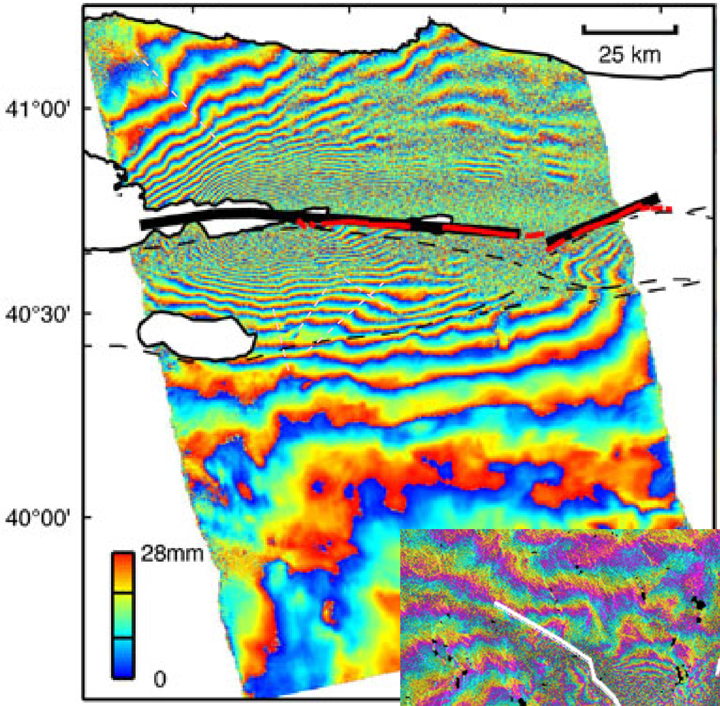

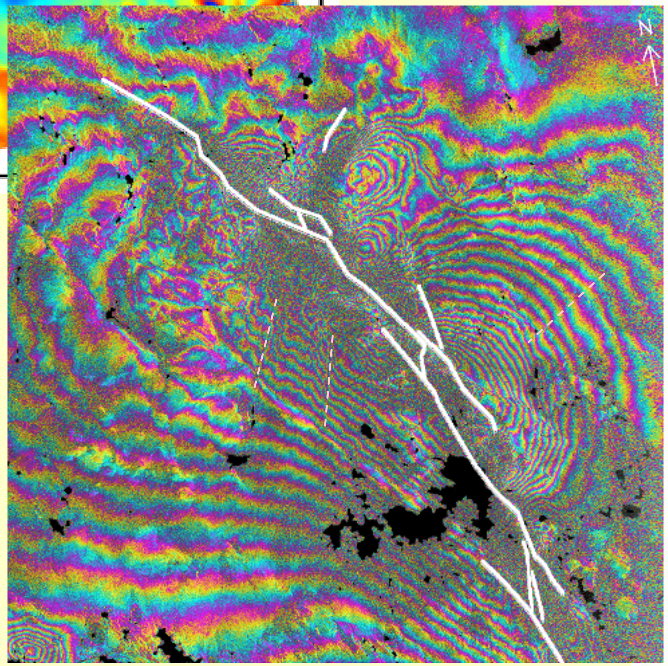

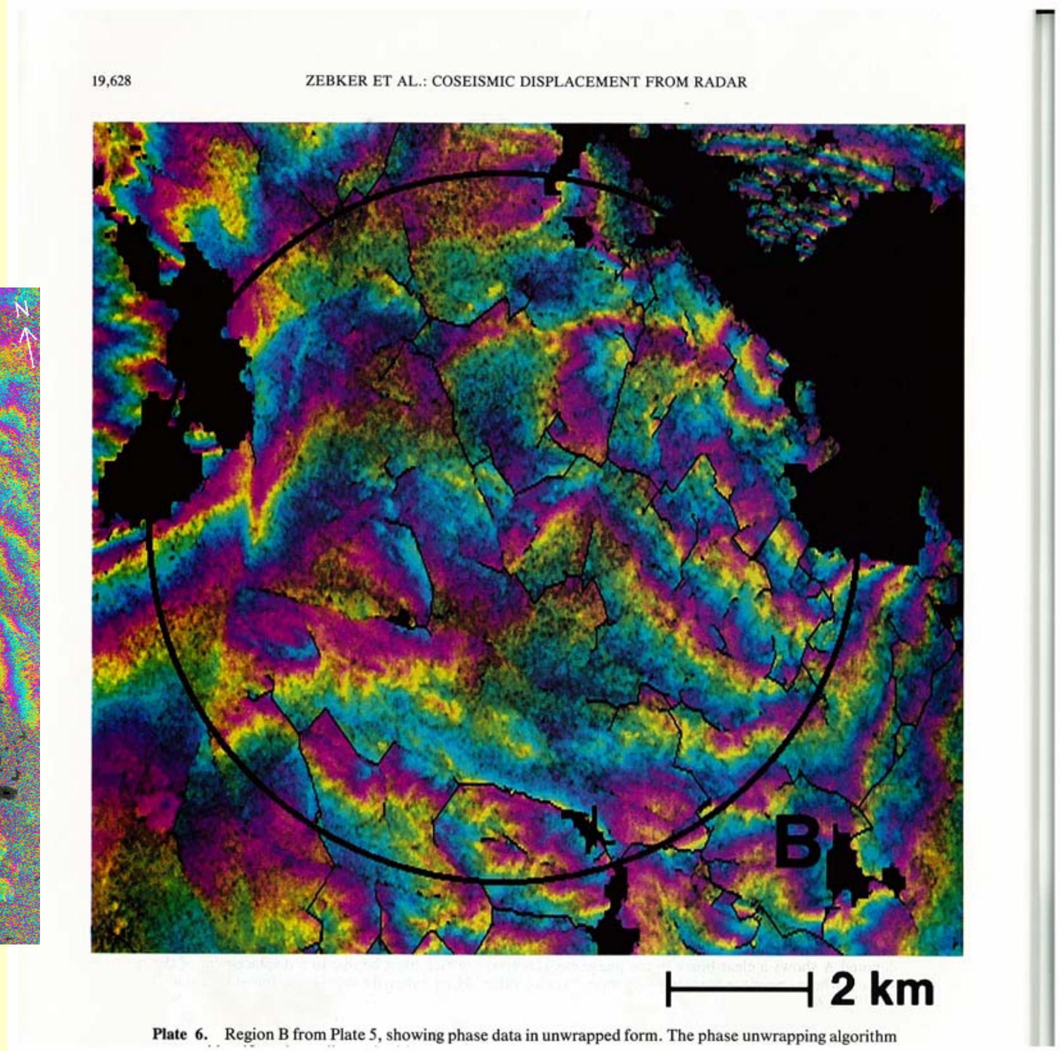
19,628 ZEBKER ET AL.: COSEISMIC DISPLACEMENT FROM RADAR

Plate 6. Region B from Plate 5, showing phase data in unwrapped form. The phase unwrapping algorithm

Part 3. On possible mechanisms responsible for properties of HF radiation

B. Deteriorated directivity: probably related to **fragmented rupture front**

Disjointed, fragmented rupture front to explain weak HF directivity:

sharp front and crack tip is possibly a LF-only concept (Gusev 1988)

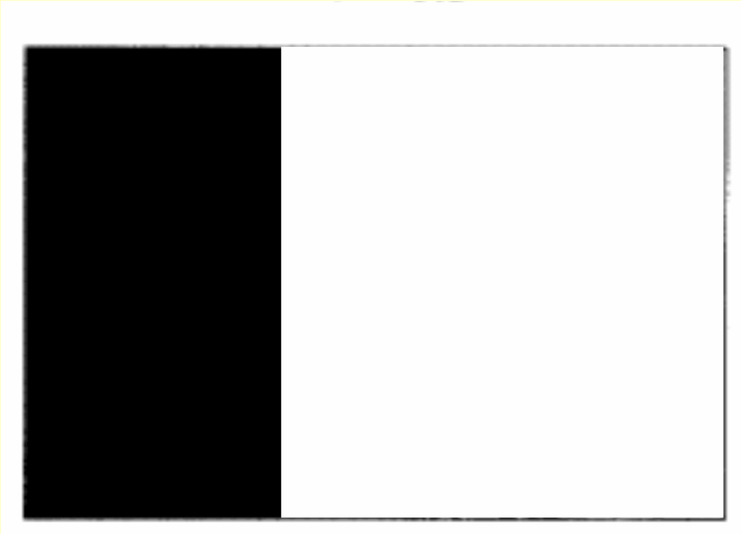

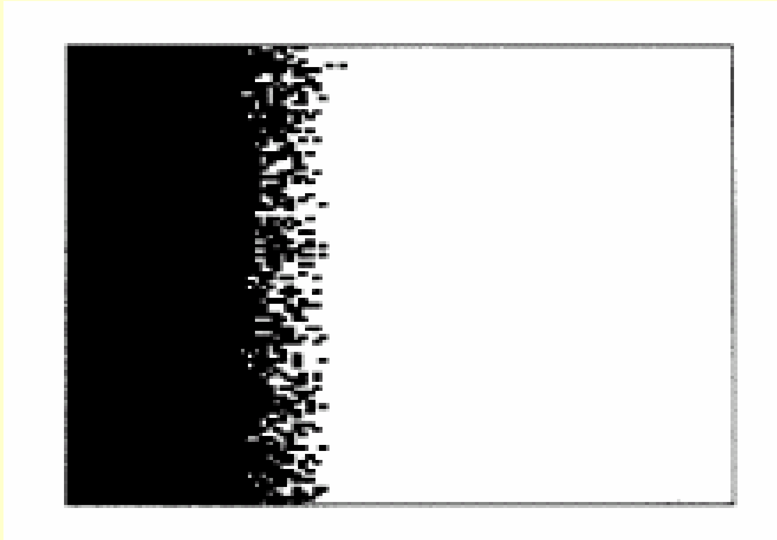

Rupture front / crack tip as ideal object and as modeling instrument at lower frequencies

Rupture front / crack tip -
more realistic representation,
may be more adequate for broad-band source description

To explain very limited HF directivity
One *needs*
incoherent, randomly phased rupture front

Illustration from
"Dynamics and Scaling Characteristics of Shear Crack Propagation"
Silberschmidt (2000)

General conclusions

(1) HF radiation bears significant information regarding earthquake fault formation and dynamics; but

(2) large part of evidence regarding HF radiation is inconclusive and not well organized.

There may be a growth point of EQ-source seismology here.

Particular conclusions

(1) In source spectra, there are two more characteristic frequencies (in addition to corner frequency); they require explanation

(2) Non-planar, rough, multiscaled fault geometry is a first candidate to explain both properties of HF energy generation and fault dynamics

ADDITIONS

Empirical spectral scaling laws (Halldorsson&Papageorgiou 2005)

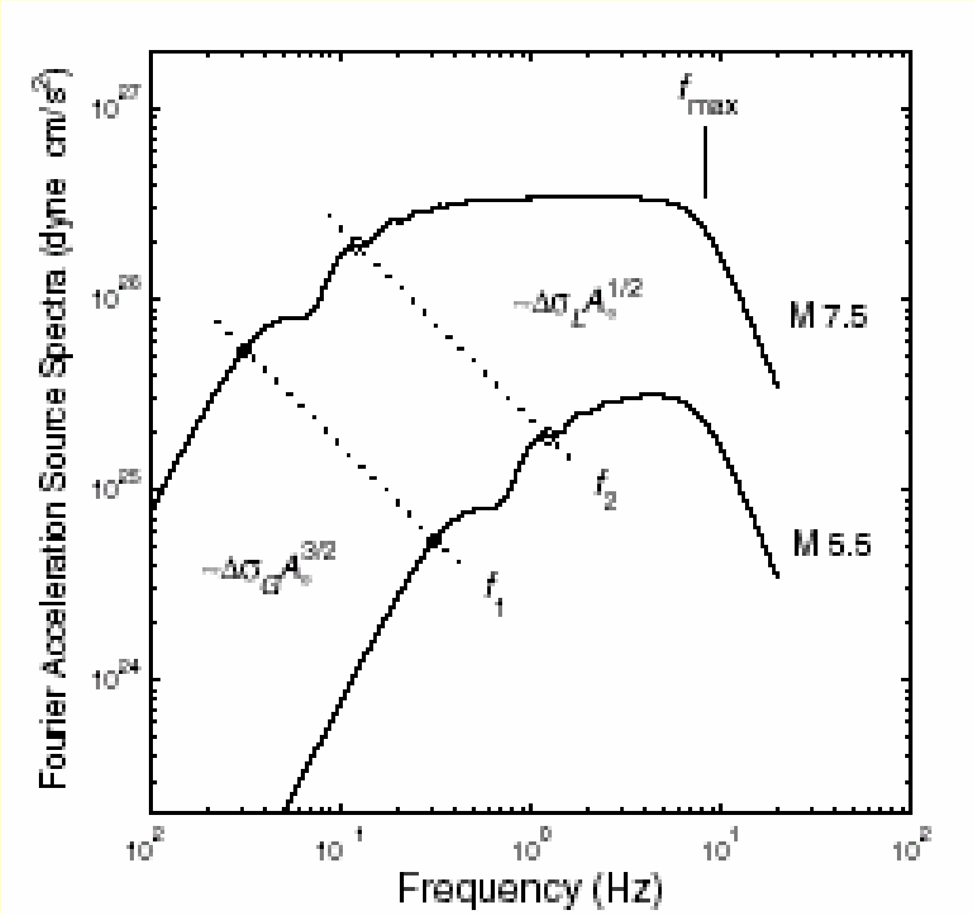

(Halldorsson&Papageorgiou 2005)

f_2 is definitively present

but is scales as f_c

Possible confusion of source-related and medium/path-related effects

- Random-like record: significant contribution from scattering is common
- Spikes: .... path effects suppress spikes
- Directivity: .... scattering reduces directivity
- Spectral shape:...... ω^{-2} *behavior*: magnitude-independent HF energy density, with important exclusion
  lack of scaling: poorly understood, may be related to non-scaling asperity statistics

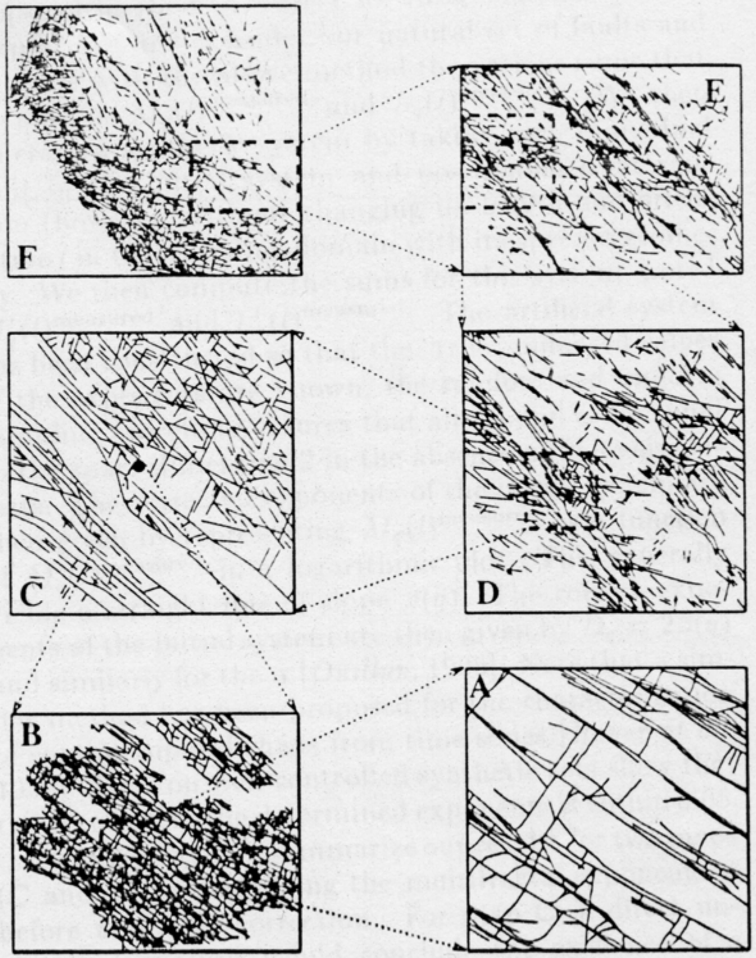

Map A: linear size=10 m, orig. scale=1:1
Map B: linear size=60 m, orig. scale=1:220
Map C: linear size=11 km, orig. scale=1:62,500
Map D: linear size=45 km, orig. scale=1:125,000
Map E: linear size=150 km, orig. scale=1:250,000
Map F: linear size=400 km, orig. scale=1:1,000,000

Figure 2. Fracture networks used in this study.

Multiscaled nature of non-planar fault geometry

Significantly deteriorated HF directivity as compared to low-frequency band (2):

Example: a_{rms} observed vs. a_{rms} calculated assuming directivity as D^p with various p

(1989 Imperial valley eq., C.-C. P. Tsai 1997)

$$D = \frac{dx/v_r}{dt} = \left(1 - \frac{v_r}{\beta}\cos\theta\right)^{-1},$$

negative evidence:

abundant empirical regressions for peak acceleration never included directivity effects

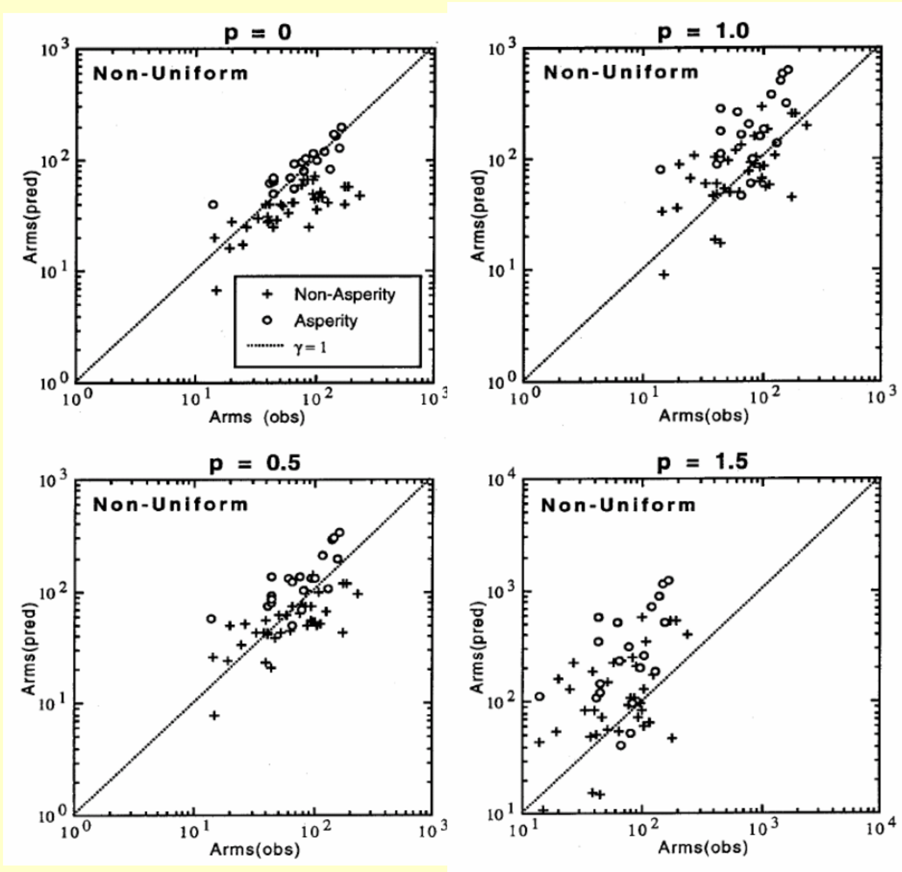

Best fit obtained with *p*=0-0.5

clearly worse fit with *p*=1, 1.5

Explanation (possible) of two acceleration spectral levels [Izutani 1984]

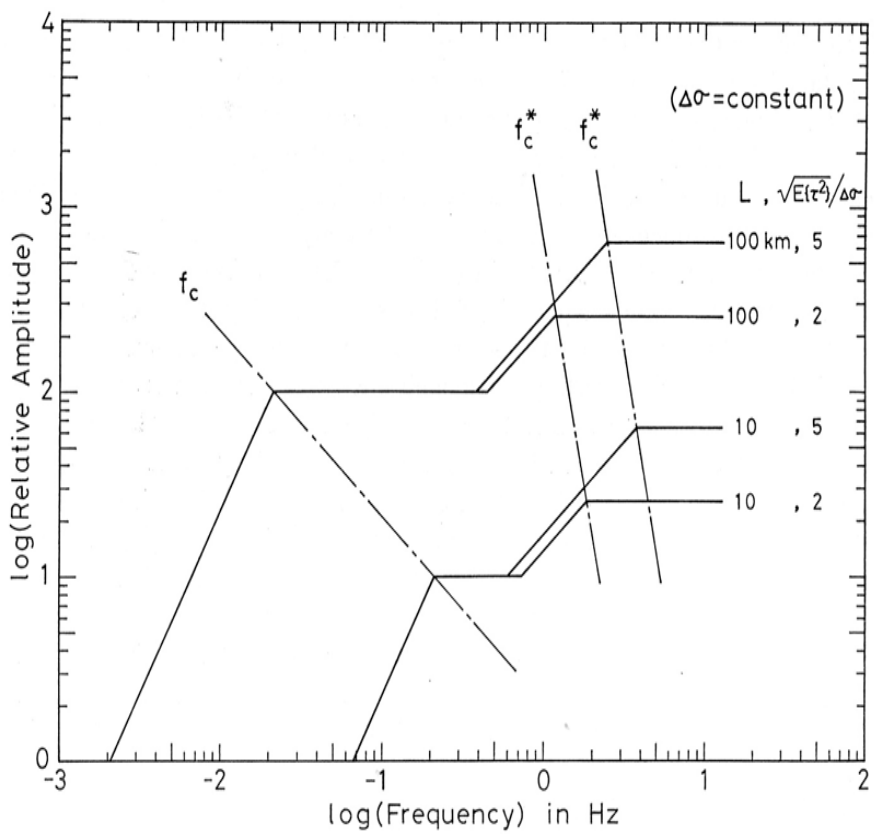

Fig. 6. Acceleration source spectra expected from the present result. The global stress-drop $\Delta\sigma$ is assumed to be constant. f_c and f_c^* are the corner frequency and the second corner frequency, respectively. L is the characteristic length of a fault plane, and $\sqrt{E\{\tau^2\}}/\Delta\sigma$ is the ratio of the rms stress-drop to the global stress-drop.

Stress drop estimate based on **HF acceleration spectrum level** is related to **RMS LOCAL STRESS DROP**

whereas stress drop based on **size-related corner frequency** is defined by **TRUE GLOBAL STRESS DROP**

These two stress drop estimates **need not be proportional to one another**

Why ω^{-2} spectral shape?

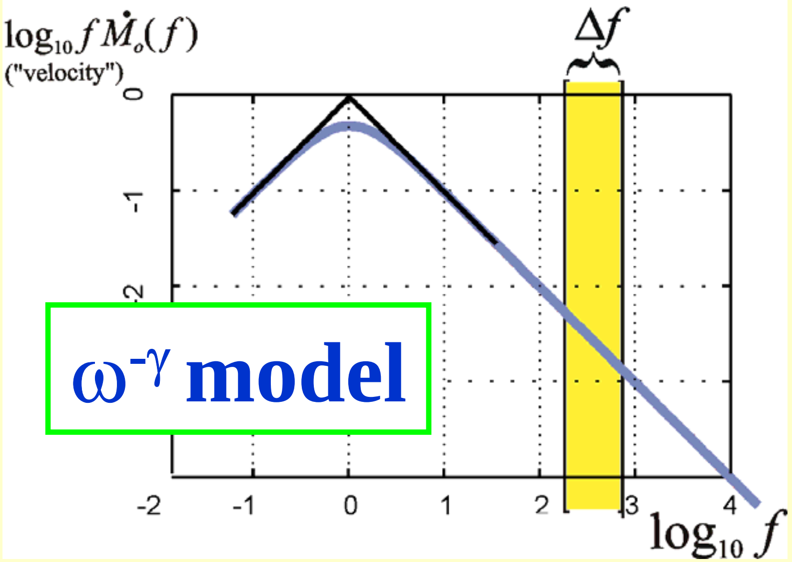

$\omega^{-\gamma}$ model

ω^{-2} model predicts
(realistically in zero approximation):
(1) flat spectral shape
(2) scaling of HF spectral level $\sim M_o^{1/3}$

$$E_s \propto \int_{f_0}^{f_0+\Delta f} \left(\frac{f M_0}{1+(f/f_c)^\gamma} \right)^2 df; \quad E_{s,HF} = E_s \big|_{f_0 >> f_c},$$

$$\left.\frac{\Delta E_{s,HF}}{\Delta f}\right|_{f_0,\Delta f} = W \propto M_0^2 f_c^{2\gamma} \propto M_0^{2-2\gamma/3} \propto S^{3-\gamma}$$

HF energy spectral density

$$\gamma = 3 \quad W \propto M_0^0 \propto \text{const}$$

$$\gamma = 2 \quad W \propto M_0^{2/3} \propto S; \qquad \leftarrow dW/dS = \text{const}$$

HF spectral luminosity

$$\gamma = 1.7 \quad W \propto M_0^{0.867} \propto S^{1.3}$$

$$E_{s,tot} \propto M_0 \propto M_0^2 f_c^3 \propto S^{3/2}$$

Spectral energy density: dE/df
Spectral luminosity: $dE/dfdS$

ω^{-2} spectra produce constant HF energy spectral density per unit area (constant *spectral luminosity*)

suggesting HF energy to be produced by the *presence* of rupture front but not by its *amplitude*